1

Soft Materials Driven by Photothermal Effect and Their Applications

*Hari K. Bisoyi[1], Augustine M. Urbas[2], and Quan Li[1]*

1 Kent State University, Liquid Crystal Institute and Chemical Physics Interdisciplinary Program, 1425 Lefton Esplanade, Kent, OH 44242, USA
2 Wright-Patterson Air Force Base, Materials and Manufacturing Directorate, Air Force Research Laboratory, Dayton, OH 45433, USA

1.1 Introduction

We are surrounded by soft materials. Most organs of the human body are made of soft materials. One defining characteristic of soft materials is that they can be readily deformed by external stimuli and stress. Even the thermal energy available at room temperature is sufficient to cause significant deformation in soft materials [1–13]. de Gennes in his 1991 Nobel lecture emphasized "flexibility" as a defining characteristic of soft materials. Colloids, polymers, liquid crystals (LCs), gels, and biological materials are categorized as soft materials. Being pervasive in nature, soft materials have been a source of inspiration for scientists and engineers for the design and fabrication of stimuli-responsive smart materials and systems for scientific investigations to understand the basic principles and technological application in devices and health care. Accordingly, a wide variety of engineered soft materials have been developed, which play a crucial role in modern technology. Soft nanotechnology, soft robotics, and soft lithography are examples that reflect the far-reaching implications of soft materials in biology and engineering [14–22]. Soft materials constitute one of the most stimulating interdisciplinary frontiers of modern science and are built on diverse experimental and theoretical foundations. Although soft materials in neat state have found a wide range of applications, fabrication of composites of soft materials by integrating other functional materials has recently become a common practice to realize advanced and tunable materials with enhanced properties for high-tech applications. Incorporation of photothermal agents into the matrices of soft materials is one such emerging approach.

Photothermal agents absorb light and convert it into heat, which is referred to as the photothermal effect. Over the past decade, many different types of photothermal agents have been reported, including inorganic nanomaterials (e.g. noble metal nanoparticles and carbon-based materials) (Figure 1.1) and organic
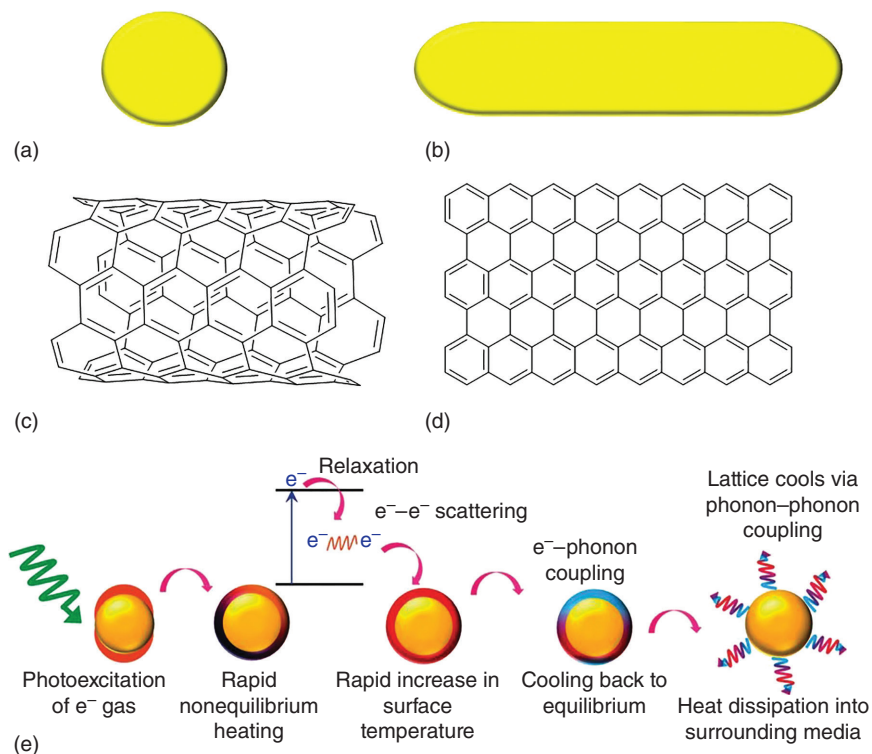
Figure 1.1 Commonly employed photothermal agents for driving soft materials by light irradiation. (a) Gold nanoparticle, (b) gold nanorod, (c) carbon nanotube, and (d) graphene. (e) Schematic describing the principle of photothermal light to heat conversion by plasmonic nanostructures. Source: Qin and Bischof [23]. Copyright 2014. Reproduced with permission from The Royal Society of Chemistry.

compounds or materials (e.g. indocyanine green and polyaniline) [23–54]. Different classes of photothermal agents are associated with their own advantages and disadvantages. Near infrared (NIR)-absorbing photothermal agents have earned a special position owing to their suitability in biological applications since biological tissues are largely transparent to NIR light. They have been applied in photothermal therapy and drug delivery remotely actuated by NIR light. Local heat produced by these agents raises the temperature and causes cell death in cancer treatment. Photothermal agents have also been used to trigger and accelerate drug release in biomedical applications. A useful photothermal agent is required to exhibit strong absorption of light and efficient transduction of light into heat. Gold nanoparticles (GNPs), gold nanorods (GNRs), carbon nanotubes (CNTs), graphene, and iron oxide nanoparticles have been employed as photothermal agents owing to their high photothermal conversion efficiency [55–67]. Similarly, conjugated polymers and dye molecules have also been utilized as photothermal agents. These organic compounds convert absorbed light through a non-radiative relaxation process. Plasmonic particles such as gold nanoparticles produce heat subsequent to light absorption through a distinct
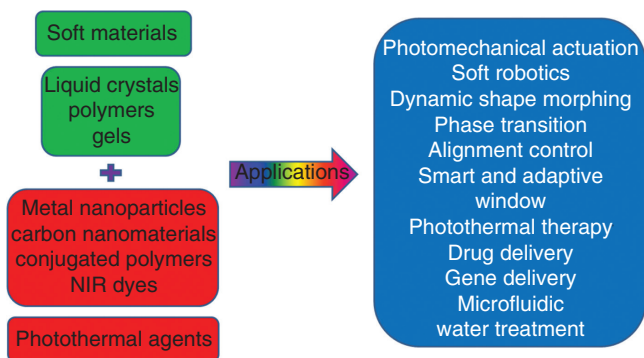
Figure 1.2 Different demonstrated applications of the hybrid systems that have been fabricated by combining soft materials and photothermal agents.

mechanism. Light absorbed by GNPs excites the electrons in the plasmonic band. These excited electrons relax through electron–phonon interaction by colliding with the gold lattice. This collision produces heat, which is transferred to the surrounding medium through phonon–phonon coupling, resulting in increasing the surrounding temperature (Figure 1.1e).

Recently, remote driving of soft materials by combining with photothermal agents is an emerging endeavor that reaps the benefits of both classes of promising materials. Accordingly, both inorganic and organic photothermal agents have been incorporated into the matrices of soft materials. The functional composite materials have been driven by light where the photothermal agent absorbs the light and converts it into heat, thereby increasing the temperature. The remotely triggered local temperature increase causes various physical and morphological changes including phase transitions. The occurrence of such changes in the soft matter matrix has been exploited for different applications (Figure 1.2). In this chapter, we present the developments on soft materials driven by photothermal effect of various photothermal agents. The combination of well-known soft materials such as LCs, polymers, and gels with inorganic nanoparticles, carbon nanomaterials, and organic dyes is discussed.

## 1.2 Liquid Crystals Driven by Photothermal Effect

Liquid crystals (LCs) represent a state of matter that appears between the crystalline solid state and isotropic liquid state [68–75]. This thermodynamically stable state of matter has been recognized as the fourth state of matter after solid, liquid, and gas. In this state of matter, the constituent elements, i.e. molecules, macromolecules, and molecular aggregates, simultaneously exhibit order and mobility, which renders it very intriguing and fascinating. The presence of order makes this state anisotropic whereas molecular mobility facilitates stimuli responsiveness. LCs are commonly known for their extensive applications in liquid crystal display (LCD) devices. However, they have been applied in numerous non-display applications [76–86]. In addition to their technological applications,

LCs are interesting for fundamental studies to understand self-assembly and self-organization of matter in multiple dimensions and over different length scales [87–97]. LCs serve as model supramolecular systems. They have been regarded as an important class of soft materials owing to their large response to small stimuli [98–108]. Moreover, they play very critical roles in living systems. LCs offer a significant contribution in nanoscience and nanotechnology. LCs have been classified into two broad classes: thermotropic and lyotropic. In thermotropic materials, the occurrence of LC phases is dependent on temperature. In lyotropic systems, the LC phase formation is primarily determined by the concentration of solutes in appropriate solvents although temperature also plays a role in the appearance and stability of LC phases.

Thermotropic and lyotropic LC phases undergo phase transition in response to the effect of temperature change. The temperature of the systems can be changed by directly heating or cooling in contact with heat sources. However, temperature variation by remote control and noncontact methods is appealing in many instances where application of direct heat is either detrimental or impractical. In this context, the use of light energy to vary the temperature of thermotropic and lyotropic LCs is very promising. In order to achieve this goal, it is often necessary to have a component in the system that can absorb the light energy and efficiently convert it into heat, thereby increasing the temperature of the medium. This role of converting light energy into heat has been played by certain metal nanoparticles, carbon nanomaterials, and organic compounds that exhibit photothermal effect. Thus, LC materials can be effectively driven by light using such photothermal agents in their matrices. The temperature variation by photothermal effect can either cause phase transitions or modification of physical properties of LC phases. Therefore, a variety of photothermal agents including inorganic nanoparticles and organic compounds have been employed for driving LC materials for fundamental studies and different applications.

Sun et al. have prepared gold-nanocrystal-doped LC elastomer microparticles and studied their light-driven shape morphing [109]. Soft lithography and polymerization techniques were used to fabricate microcylinders from the LC elastomer nanocomposite. The processing conditions were such that weakly undulating director orientation along the long axis of the microcylinders was obtained. Upon irradiation with infrared (IR) laser, the dispersed GNPs efficiently produce heat and transfer it to the surrounding in the matrices. This local heat produced upon exposure to IR light is able to modulate the ordering in the liquid crystalline microparticles. Both reversible and irreversible changes in the shape of the microcylinders have been observed using scanned beams (Figure 1.3).

Fong et al. doped GNRs into a lyotropic LC matrix [110, 111]. Through NIR laser irradiation, they could achieve control over the nanostructure of the mesophase (Figure 1.4). Since lyotropic mesophases are used for drug and gene delivery applications, control over their nanostructures could facilitate on-demand delivery of encapsulated agents. Integration of GNRs and driving phase transitions by photothermal effect in lyotropic mesophases are promising way to control the nanostructure of the mesophases. Accordingly, GNRs were dispersed into the lyotropic mesophase matrix and the reversible changes in their nanostructures under NIR laser irradiation were investigated by different techniques.
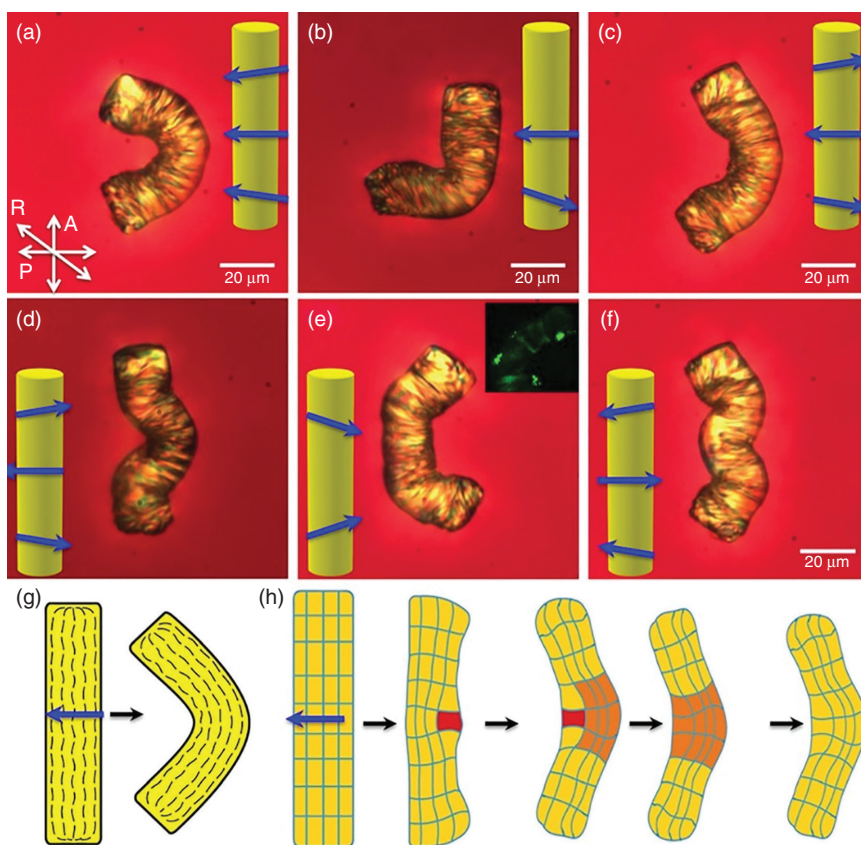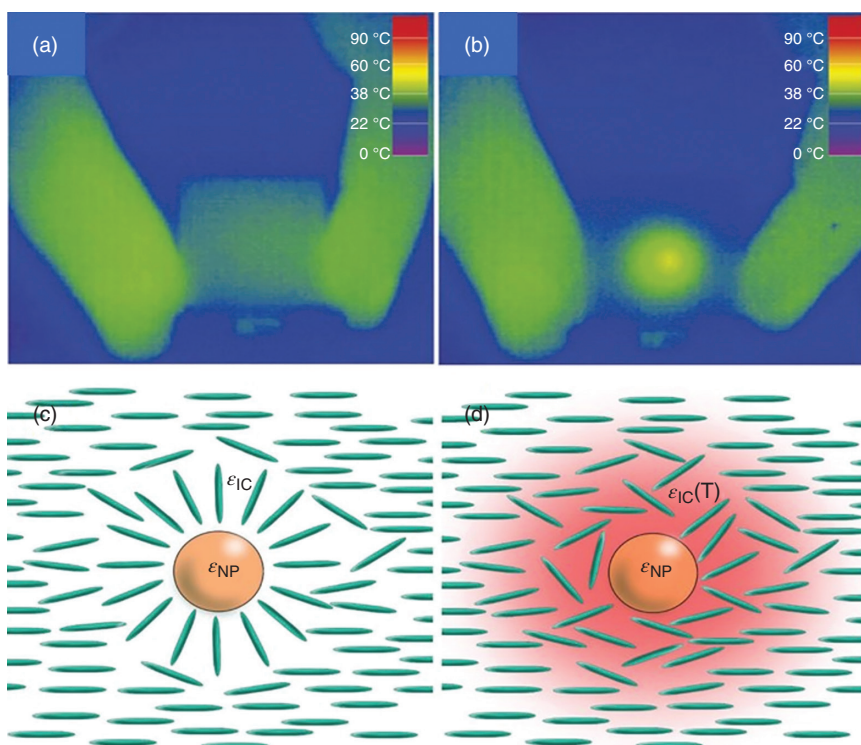
Figure 1.3 Examples of robust reversible morphing of liquid-crystalline elastomer (LCE) microparticle shapes by means of unidirectional laser beam scanning along blue arrows shown in the insets of (a–f). The inset in (e) shows a typical CARS-PM image of a microparticle that was bent using a scanning laser beam. (g) Schematics of transformation of weakly undulating director field ($n(r)$) (shown by dashed lines) as the particle is bent due to scanning. (h) Schematic drawings show the effect of local manipulation of LCE orientational ordering by a scanned laser beam along the direction marked by the blue arrow; the scanning causes nonreciprocal unidirectional motion of a molten region (red) and in modification of the LCE polymeric network in the vicinity of the "hot" scanning region (orange), eventually leading to the stable modification of the particle shape that persists after the laser is turned off. Source: Sun et al. 2012 [109]. Copyright 2012. Reproduced with permission from the American Institute of Physics.

Moreover, the effects of lipid composition, aspect ratio, and concentration of GNRs as well as laser pulse duration on the response of the systems were studied.

Fong et al. further undertook studies to understand the role of photothermal effect in non-lamellar LC systems [112]. They set out to reveal the photothermal response of known and new lamellar and non-lamellar lyotropic phases by correlating the thermal properties of the materials and the photothermal energy conversion by the photothermal agent. Photothermal heating was carried out by irradiating the composite systems with NIR laser and the consequent structural

Figure 1.4 (Top) The molecular structures of phyt and GMO. In excess water, the two lipids transition from the double diamond bicontinuous cubic phase (v2D) to the inverse hexagonal phase (H_2), and then the fluid isotropic inverse micellar phase (L_2) with increasing temperature. (Bottom) The observed phase transition of the phyt-GNR LC upon laser irradiation. On irradiation, the phyt-GNR LC transitioned from v2D to H_2 to L_2, and on cessation transitioned back from L_2 to H_2 + the nonequilibrium gyroid bicontinuous cubic phase, v2G, before returning to v2D. Source: Fong et al. 2012 [110]. Copyright 2012. Reproduced with permission from The American Chemical Society.

changes of the LC phases were monitored by X-ray scattering studies. The effect of GNRs on the hexagonal phase was studied by electron microscopy techniques. Detailed understanding of such lyotropic nanocomposites is critical for their use in drug delivery applications remotely triggered by photothermal effect.

Pezzi et al. studied the photothermal effect of GNPs in thermotropic nematic liquid crystal (NLC) phases both experimentally and theoretically [113]. They characterized the photothermal effect of GNPs doped into thermotropic LCs and subsequently modeled the observations. Theoretical modeling of the pho-toinduced temperature variation in the LC nanocomposites was performed using the thermal heating equation that is applicable to an anisotropic medium such as the host nematic phase. Predictions of the theory were verified by conducting photothermal experiments on an LC nanocomposite fabricated by dispersing GNPs into a nematic host. Thermographic comparison between the nanocomposite and pure host clearly shows that GNPs are responsible for the observed photothermal effect under resonant optical frequency (Figure 1.5). This comprehensive investigation contributes toward the understanding of the physical phenomenon of heat propagation at the nanoscale.

Liu et al. observed rapid and reversible actuation of LC elastomer micropillars containing GNPs [114]. In this study, a new experimental protocol has been

Figure 1.5 (a, b) Thermographic analysis of the sample under optical irradiation for the pure NLC (a) and NLC/GNP (b) cell. (c, d) Sketch of the GNP dispersed in the NLC without and with heating respectively. Source: Pezzi et al. 2015 [113]. Copyright 2015. Reproduced with permission from The Royal Society of Chemistry.

developed to facilely disperse GNPs and GNRs into the polyacrylate-based LC elastomer. Micropillars and microactuators containing GNPs and GNRs were fabricated from the plasmonic polymer nanocomposites. The effect of the incorporated GNPs was investigated by a battery of characterization methods including microscopy, spectroscopy, thermal analysis, and scattering experiments. Photothermal actuation behavior of the composites and the pure elastomer host were studied and compared. It was found that GNR is a good candidate for the development of LC elastomer-based high-performance photothermal actuators. Yang et al. prepared GNR-containing LC elastomer composites using thiol-click chemistry [115]. These elastomeric composites exhibited responsiveness to NIR and underwent nematic to isotropic phase transition under NIR irradiation.

We designed and synthesized mesogen-functionalized plasmonic GNRs and dispersed them into thermotropic NLC hosts [116]. Mesogen functionalization of the nanorods enhanced their compatibility in the LC matrix and enabled their homogeneous dispersion. Upon irradiation with NIR laser, the LC nanocomposite exhibited nematic to isotropic phase transition (Figure 1.6). However, when the light source was turned off the mixture returned back to the nematic phase. Thus, reversible phase transition was observed in the nanocomposites. It was noticed

(a)

(b)
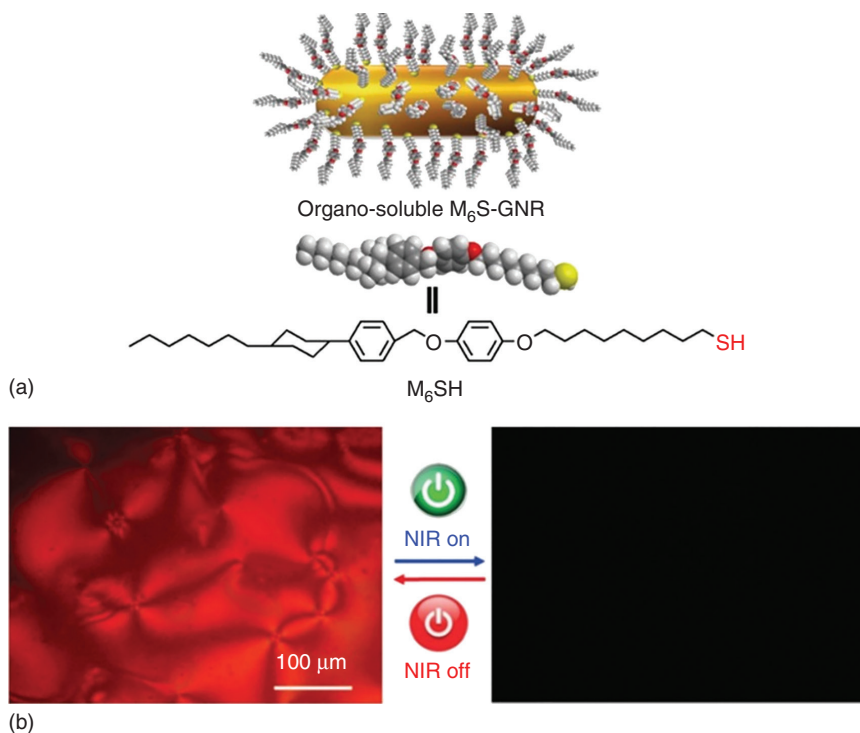
Figure 1.6 (a) Mesogen-functionalized organosoluble GNR. (b) Phase transition of the 0.5 wt% M_6S-GNR/E7 composite at DT = 3 1C with NIR laser irradiation took approximately two seconds from the nematic to the isotropic phase whereas it took approximately one second to return from the isotropic to the nematic phase when the NIR light was turned off. Source: Gutierrez-Cuevas et al. 2015 [116]. Copyright 2015. Reproduced with permission from The Royal Society of Chemistry.

that composites containing higher concentration of mesogen-functionalized GNRs underwent faster phase transitions.

Pezzi et al. found that GNPs embedded in NLCs exhibit a photothermal effect that is dependent on the refractive index of the medium [117]. They implemented a theoretical model to account for the observed photoinduced temperature variations in GNPs dispersed in NLCs. Experimental results of GNP LC composites have been compared with the theoretical predictions. de Sio et al. have studied plasmonic heating of GNRs in chiral LCs [118]. It was found that the presence of GNRs desensitizes the shift of the cholesteric liquid crystal (CLC) reflection band to temperature. Suitable cell design enables one to "turn off" the wavelength shift of the peak reflection, thereby turning the system into a pure amplitude measurement tool.

We have achieved handedness inversion in a GNR containing a CLC phase driven by NIR light irradiation [119]. Mesogen-functionalized GNRs were dispersed into the CLC phase formed by a chiral mesomorphic compound. Upon NIR irradiation, the sample temperature increases due to the photothermal effect of GNRs, which brings about pitch changes in the cholesteric system and

thus a change in the selective reflection. Interestingly, the cholesteric system exhibits handedness inversion upon increasing the temperature (Figure 1.7). Red, green, and blue reflection colors were obtained both in the right- and left-handed states of the CLC. This NIR-light-driven plasmonic system would be
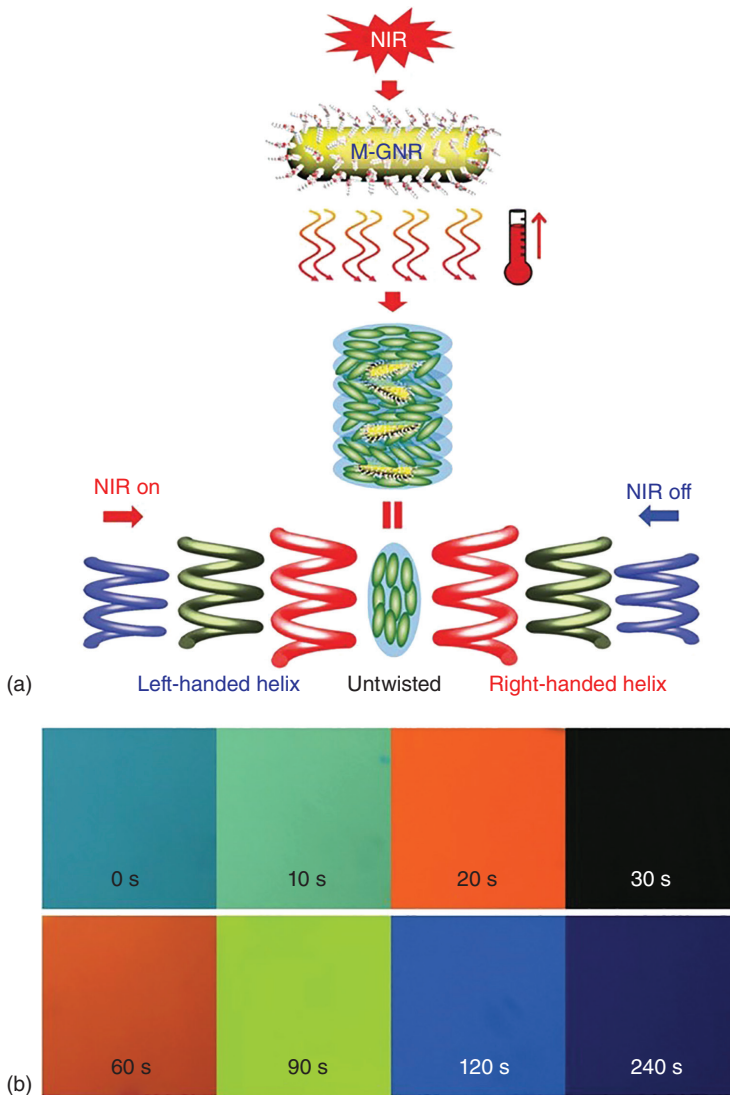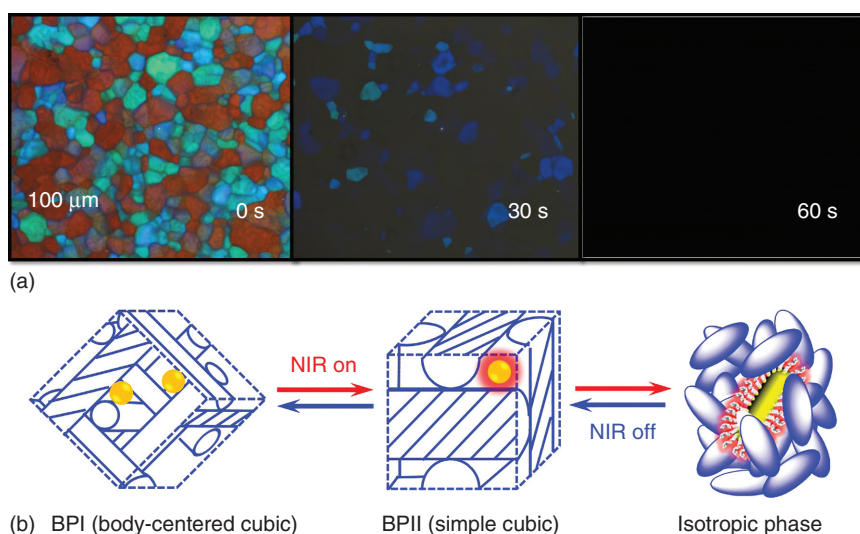

Figure 1.7 (a) Schematic illustration of NIR-light-directed handedness inversion in mesogen-grafted GNR (M-GNR)-embedded helical superstructure resulting from the "photothermal effect" of the plasmonic nanorods. (b) Dynamic photonic reflection colors of self-organized helical superstructure loaded with 0.2 wt% 770 nm M-GNRs in a 10-μm-thick planar cell upon NIR laser irradiation at 808 nm, taken under a crossed polarized optical microscope in reflection mode. Source: Wang et al. 2016 [119]. Copyright 2015. Reproduced with permission from Wiley-VCH Verlag GmbH & Co. KGaA.

promising in applications where both left- and right-handed circularly polarized light with tunable wavelengths are required.

We have also utilized the photothermal effect of GNRs to study phase transitions in LC blue phase composites [120]. Mesogen-functionalized GNRs were designed, synthesized, and dispersed into the cubic matrix of a blue phase. Upon irradiation with NIR light, the composite exhibited phase transition from a body-centered cubic lattice to a simple cubic lattice before turning into the isotropic phase. The NIR-light-driven phase transition has been found to be reversible (Figure 1.8). Interestingly, the lattice constant of the blue phase could be tuned by NIR light irradiation, which has produced red, green, and blue reflection colors from these photonic nanostructures.

Palermo et al. have demonstrated optical control of the plasmonic heating effect in NLCs employing the photoalignment technique [121, 122]. Here, they have exploited the dependence of the refractive index of NLCs on the molecular orientation. By varying the molecular alignment of the NLCs, control over the rate of plasmonic heating by the GNPs has been achieved.

Yang et al. have reported IR-light-driven reversible actuation in LC elastomer nanocomposites containing CNTs [123]. They used poly(p-phenyleneethynylene)-functionalized single-walled CNTs as fillers in the LC elastomer matrix. Such functionalization was found to enhance the dispersibility of CNTs in the elastomer matrix. The NIR response of the composite was found to increase upon high loading of CNTs in the composites. Ji et al. have developed a protocol for the dispersion and alignment of CNTs in LC polymers and elastomers [124].


Figure 1.8 (a) Typical polarized optical microscope (POM) images of blue phases (BPs) doped with 0.3 wt% M-GNRs in 10-mm-thick untreated cells upon irradiation with an 808-nm NIR laser (2 W). (b) Schematic illustration of the NIR-light-tunable self-organized soft photonic superstructures. The yellow dots represent the cross section of GNRs in the BP matrices. Source: Wang et al. 2015 [120]. Copyright 2015. Reproduced with permission from The Royal Society of Chemistry.

They have taken advantage of the photothermal property of the embedded CNTs to achieve remote-controlled actuation of the elastomeric nanocomposites. Li et al. demonstrated actuation of LC elastomer nanocomposites containing CNTs driven by IR as well as white light [125]. Similar observations have been reported by Marshall et al. [126]. Direct sunlight has also been employed to drive LC elastomer nanocomposites containing CNTs [127].

Kohlmeyer and Chen fabricated and demonstrated wavelength-selective IR-light-driven hinges based on LC elastomers [128]. Composites of the elastomers were prepared by dispersing either CNTs or NIR dyes. The elastomeric nanocomposites exhibit fast and reversible bending upon NIR light irradiation. Bilayers films and inchworm walkers have been realized using these nanocomposites (Figure 1.9).

Li et al. reported bulk nanocomposites from LC elastomers and single-walled CNTs [129]. Light-driven bulk actuation in the composites was demonstrated under uniform as well as asymmetric irradiation. Wang et al. have synthesized polysiloxane-based LC elastomers containing azobenzene moieties [130]. Nanocomposites prepared from these elastomers can be driven either by NIR or by UV irradiation. NIR laser irradiation was found to cause shrinkage of the nanocomposite films.

Yu et al. fabricated polymer-dispersed LC–graphene oxide nanocomposites and prepared thin films using the solution casting method and mechanical stretching [131]. In the composites, graphene-oxide-doped poly(vinyl alcohol) acted as the matrix whereas a low molar mass room temperature NLC formed
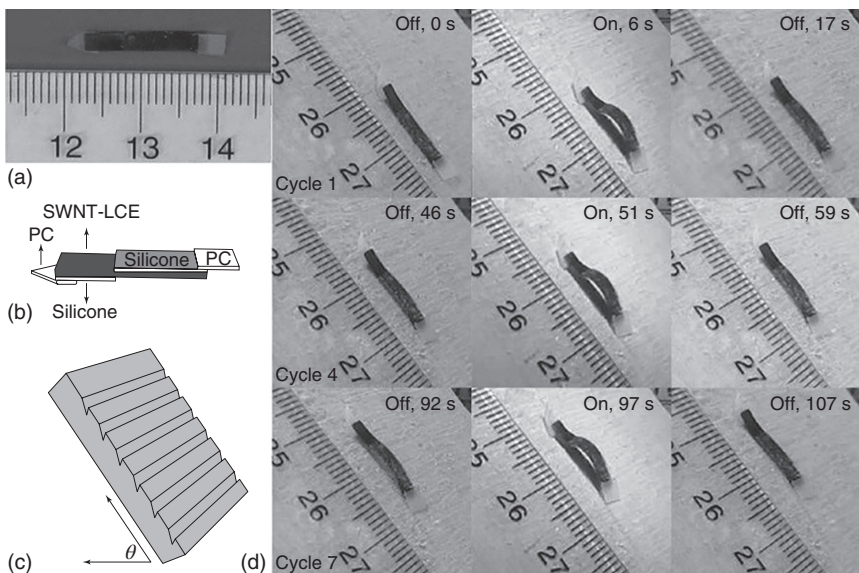

Figure 1.9 (a) Photograph and (b) scheme of an inchworm walker device consisting of an asymmetric SWNT-LCE/silicone bilayer film. (c) Scheme of a ratcheted wood substrate. (d) The inchworm walker crawling up the wood substrate at a 50° incline in response to on and off cycles of CW NIR light (28.2 mW mm^{-2}). Source: Kohlmeyer and Chen 2013 [128]. Copyright 2013. Reproduced with permission from Wiley-VCH Verlag GmbH & Co. KGaA.

a separated phase. The nanocomposite films exhibited photomechanical response upon irradiation with visible light (Figure 1.10a–c). The origin of this response has been attributed to arise from the photothermal effect of graphene oxide.

Yu et al. further demonstrated light-driven tumbler movement in polymer graphene oxide nanocomposite films [132]. Reversible and stable photomechanical behavior was obtained in these nanocomposites due to the combination of shape memory effect of the polymer host and photothermal effect of the graphene oxide guest. Control over such complicated motion could lead to devices with improved performances.

Quinn et al. have dispersed graphene nanoparticles into lyotropic LC phases [133, 134]. They observed that upon NIR light irradiation, the lyotropic system undergoes phase transition from cubic to micellar through hexagonal phase (Figure 1.10d). The cubic phase recovers when the NIR source is removed. The occurrence of reversible phase transition has been attributed to the local heating of the matrix through photothermal effect of the embedded graphene particles.
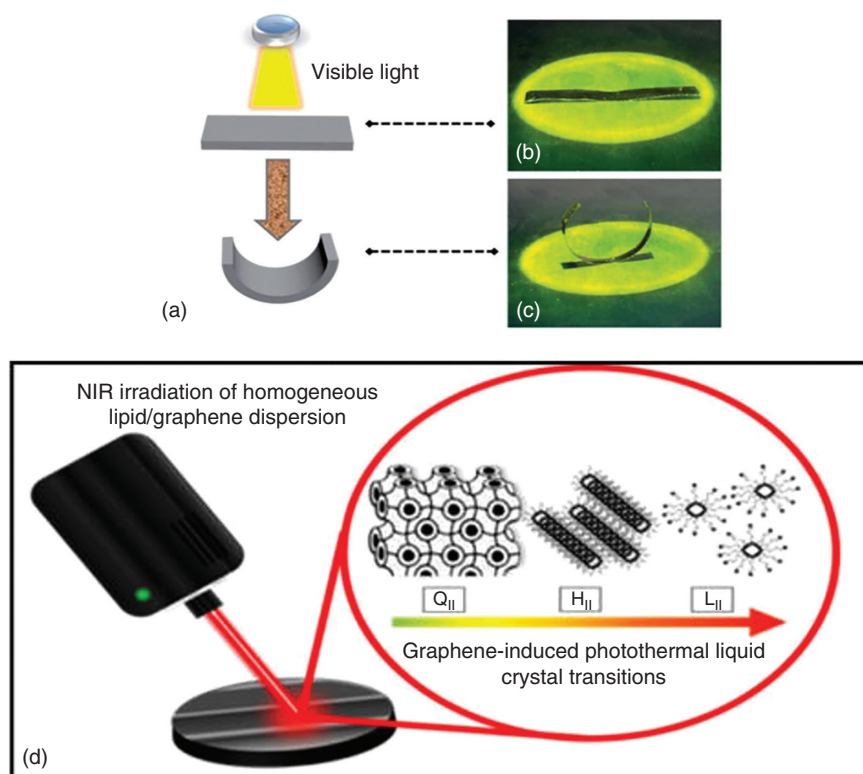
Figure 1.10 Visible-light-responsive behavior of the stretched polymer-dispersed liquid crystalline/graphene oxide (PDLC/GO) nanocomposite films. (a) Schematic illustration of photomechanical behaviors. (b) and (c) Photographs of the nanocomposite films before and after irradiation with visible light. (d) Schematic diagram showing the change in phase upon photothermal heating of the phytantriol–water LC. Source: Xiang et al. 2015 [131]. Copyright 2014. Reproduced with permission from The Royal Society of Chemistry. Yu et al. 2014 [101]. Copyright 2015. Reproduced with permission from The American Chemical Society.

Such hybrid systems could be employed for *in vivo* payload release by stimulation with NIR irradiation.

Yang et al. have prepared LC elastomer nanocomposites containing graphene nanosheets by *in situ* photopolymerization [135]. Photopolymerization and hot-drawing of the composites have yielded composites with highly aligned graphene in their matrix. They have investigated the photomechanical actuation in nanocomposite films driven by NIR irradiation (Figure 1.11).

Li et al. have observed substantial light-induced uniaxial contraction in LC elastomer nanocomposites containing graphene oxide nanoparticles [136]. Moreover, photoactuation of the nanocomposites has been observed under both UV and IR light irradiation.

Wang et al. have synthesized mesogen-functionalized graphene, which facilitates homogeneous dispersion and high compatibility in a chiral LC matrix [137]. Utilizing the stable LC nanocomposites, an adaptive window system has been demonstrated that responds to multiple stimuli (Figure 1.12). The optical transparency of the device could be modulated between transparent and opaque states by IR light irradiation by exploiting the photothermal effect of graphene sheets incorporated into the system. Here, light-induced heating of the film causes phase transition in the chiral LC, leading to transparency modulation. The chiral nanocomposites hold huge potential toward the fabrication of adaptive and energy-efficient windows for automotive and architectural applications.

Vallooran et al. have introduced magnetic nanoparticles into the matrix of lyotropic LCs and investigated the photothermal effect of the nanoparticles on the phase behavior of the system [138]. The magnetic nanoparticles greatly facilitate the alignment of the LC phase under magnetic field. Upon photoirradition, the system was observed to undergo LC to isotropic phase transition owing to the photothermal effect exhibited by the iron oxide nanoparticles. It was found that the effect of the photothermal effect could be tuned by adjusting
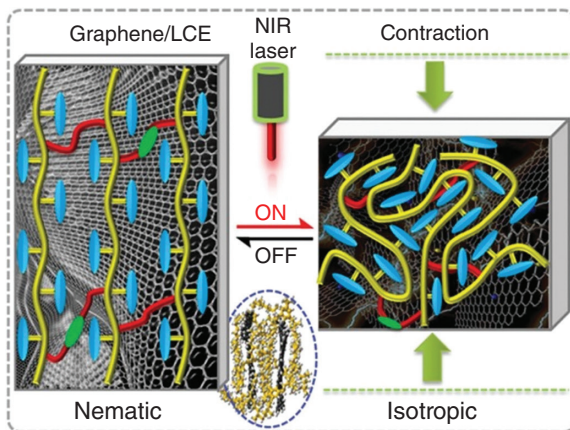
Figure 1.11 Schematic illustration of reversible photomechanical actuation in graphene/LCE nanocomposites upon an on–off switching of NIR light. Source: Yang et al. 2015 [135]. Copyright 2015. Reproduced with permission from Wiley-VCH Verlag GmbH & Co. KGaA.
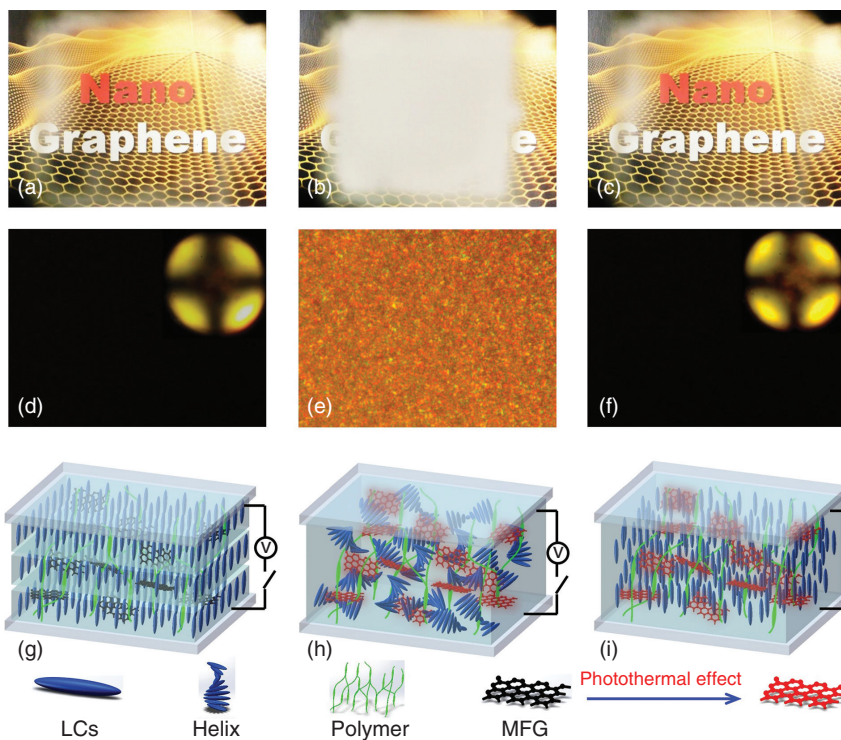
Figure 1.12 Polymer-stabilized MFG-containing chiral LC thin film. Photograph of the polymer-stabilized MFG-containing chiral LC film with 7 wt% R811: (a) transparent state at room temperature; (b) opaque state after NIR irradiations (2 W); (c) transparent state from the unwound cholesteric focal conic phase upon applying the electric field. POM images of the devices under different addressing conditions (d–f). Schematic illustrations of the corresponding configurations of LC phases (g–i) in the devices. Source: Wang et al. 2017 [137]. Copyright 2017. Reproduced with permission from Elsevier.

the concentration of the nanoparticles in the matrix. Moreover, the orientational order can also be modulated by changing the concentration of the particles. This hybrid mesophase system is responsive to both magnetic field and photoirradiation.

Ono and Kawatsuki have studied the photothermal response characteristics of host–guest LC systems [139]. The results showed the photoresponsive properties to be dependent on the change in refractive index of the system due to temperature variation caused by laser light absorption. It was noticed that refractive index change was proportional to laser beam intensity. The photothermal response of the system was reversible. They have further investigated photothermal effect in NLCs on a dye-doped polymer film [140]. The NLC molecules were found to undergo reorientation due to rise in temperature at the interface between the NLC layer and the polymer surface.

Guo et al. have fabricated and investigated NIR-absorbing elastomer composites containing mesogenic croconaine dye [141]. They designed and synthesized the first example of an NIR-absorbing liquid crystalline croconaine-based dye.

The LC nature of the NIR dye makes it more compatible in the elastomer matrix. Moreover, homogeneous distribution of the dispersed dye could be achieved in the soft polymer matrix. A monodomain LC elastomer composite was obtained by adopting the traditional LC alignment method in combination with photopolymerization of monomer mixtures. Films fabricated from the elastomer composite were able to show a fully reversible contraction and expansion cycle in response to NIR light irradiation. Liu et al. have dispersed polyaniline-conducting polymer nanoparticles into the matrix of LC elastomers and investigated their NIR response through photothermal effect [142]. The effect of doping concentration and the conjugation form of the polyaniline nanoparticles on the photomechanical response of the elastomer composite was studied. The elastomeric composite material was found to exhibit fully reversible muscle-like actuation and could lift up heavier weights under NIR irradiation owing to the photothermal effect of the polyaniline nanoparticles.

Gelebart et al. have reported on self-sustained mechanical oscillators that are produced by embedding NIR-absorbing dyes into LC networks [143]. They developed splay-aligned LC networks using commercially available LC monomers. To obtain self-sustained oscillation in the system by light irradiation they have added photostabilizers into the polymer network matrix that convert absorbed light into heat through non-radiative relaxation. The observation of mechanical self-oscillation has been linked to temperature variation over the film thickness. The oscillation of a beam-shaped device (Figure 1.13) is activated in a localized responsive zone that acts as a hinge. It was found that light spanning across UV to the NIR region could be employed for actuation.

Liu et al. synthesized NIR chromophore-functionalized LC elastomers that are capable of exhibiting fast response speed and promising mechanical property [144]. A croconaine dye-based cross-linker was used as the NIR-absorbing motif. They prepared uniaxially aligned main-chain LC elastomers using a two-step diene metathesis *in situ* polymerization and cross-linking. Under NIR irradiation, the elastomer system raises its temperature from 18 to 260 °C by efficient photothermal conversion due to the presence of homogeneously distributed and covalently linked NIR chromophore. The soft actuator fabricated from these NIR-absorbing elastomers was able to lift loads 5600 times heavier than its own weight.

Li et al. have doped polydopamine nanoparticles into the matrices of LC elastomers. The photothermal effect of polydopamine has been exploited in the systems for developing dynamic three-dimensional (3D) structures by light-irradiation-induced deformations [145]. The dispersion of polydopamine in the elastomer matrices turned out to be more facile than the dispersion of CNTs. The mechanical properties of the polydopamine-dispersed elastomers have been found to be superior to those of the pure host materials. Tian et al. have reported the fabrication and light-driven actuation of polydopamine-coated LC elastomers [146]. These coated systems exhibit rapid response and significant contraction because of the photothermal effect of polydopamine cladding. Interestingly, by surface scanning with NIR laser the polydopamine-coated elastomer films could be made to bend or roll up. A prototype robotic swimmer was designed and demonstrated using the elastomer films, which was able to swim
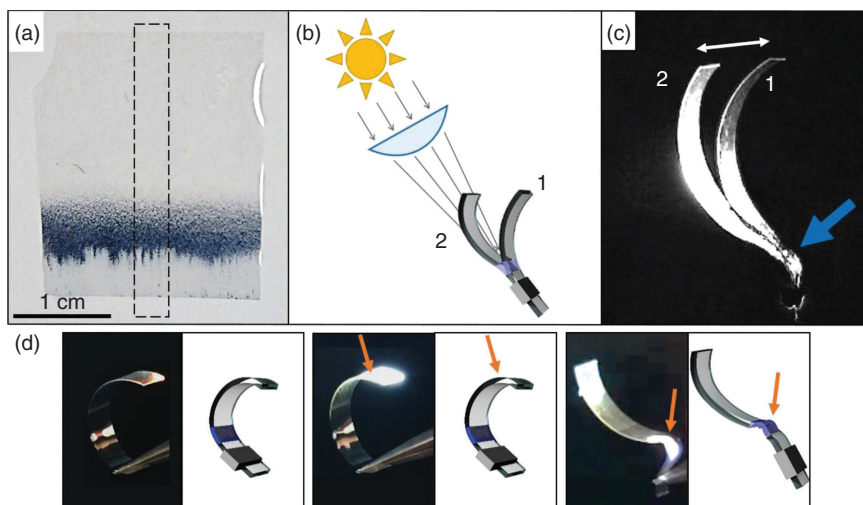
Figure 1.13 Self-oscillation obtained with the indigo hinge. (a) Picture of the nonactive film with the hinge of indigo component. (b) Schematic representation of the setup used to actuate the liquid crystalline network (LCN) film containing a stripe of indigo. The sunlight is focused by a lens and has sufficient intensity to bring the system into an oscillating mode, between positions 1 and 2. (c) Superposition of two pictures of the oscillating film in positions 1 and 2. Over time, the film is moving continuously between these two positions. The self-shadowing at the hinge is visible in this superposition. In position 1 the hinge is in the shadow while it is in the sunlight in position 2. (d) In the first picture, the film is in the dark at the resting state. In the second picture, the focus point of the light (indicated by the orange arrow) does not overlap with the indigo stripe and no bending is observed. In the last picture, the film is positioned so that the focused light reaches the indigo stripe. In that condition only, the film bends significantly and self-oscillates. Source: Gelebart et al. 2017 [143]. Copyright 2017. Reproduced with permission from Wiley-VCH Verlag GmbH & Co. KGaA.

on the water surface in response to NIR laser irradiation. The above-described research shows that polymer-based photothermal agents could be employed in the fabrication of optically driven artificial muscle for application in soft robotics and functional optomechanical devices.

1.3 Polymers Driven by Photothermal Effect

Biopolymers such as polysaccharides, polypeptides, and polynucleotides have played a vital role in the evolution and advance of life. Their criticality in life process is well appreciated by scientists and nonscientists alike. Synthetic polymers such as teflon, nylon, and polyesters have revolutionized the way we use materials and have significantly influenced our modern life, starting from the comfortable clothes we wear to the luxury cars we drive. Very recently, supramolecular polymer materials have been developed by appropriate engineering of different noncovalent interactions. These dynamic and functional materials display a variety of promising properties and enable many applications that are either difficult or impossible to achieve by conventional polymer materials.

While polymers themselves are interesting, recently it has been recognized that their composites often exhibit remarkably superior traits and perform better in certain applications. Accordingly, many varieties of polymer composites have been developed and explored, and in the recent years polymer nanocomposites containing CNTs, graphene, and graphene derivatives have been paid special attention [147–152]. It has been noticed that carbon-based nanomaterials often enhance the optical, electrical, and mechanical properties of polymer nanocomposites and introduce new capabilities into the hybrid polymer systems.

CNTs, which absorb light and convert it into heat, have been dispersed into the matrices of various polymers to realize functional polymer nanocomposites. The polymer matrices can be driven by the photoinduced temperature increase [153]. CNTs have been used in thermoplastic elastomer matrices for efficient shape recovery by utilizing the photothermal effect of CNTs that facilitates local heating in the system upon light irradiation. Ahir et al. investigated IR-light-induced actuation in aligned polymer–nanotube composites [154, 155]. The polymer–CNT composites have been found to either expand or contract depending on the processing of the hybrid system. Rubber composites with multi-walled CNTs have been prepared and their reversible photomechanical actuation response has been investigated under NIR light irradiation. CNTs were aligned in the rubber matrix by applying stress to the composites. The degree of alignment of the nanotubes was found to influence the photomechanical response of the composites. These composites contract along the alignment direction of the nanotubes. Different polymer hosts were evaluated to gain greater insight into the photomechanical actuation triggered by NIR light.

Lu and Panchapakesan investigated the photomechanical responses of CNT/polymer actuators [156]. They compared the photomechanical response of bulk polymer nanocomposites and multilayer constructions containing single-walled CNTs and multi-walled CNTs. The photomechanical actuation behavior of the composites containing single-walled CNT and multi-walled CNT was related to nanotube alignment in the matrix and the presence of pre-strain. Comparable actuation properties were observed between multilayered constructions and bulk composites. Expansion and contractions were observed under small and large pre-strains respectively. Miyako et al. fabricated and studied CNT–polymer composites for light-driven microthermal control [157]. Here, polydimethylsiloxane (PDMS) was chosen as the soft polymer and noncovalently surface-functionalized CNTs were dispersed into its matrix. Noncovalent functionalization of CNTs is often preferred since this procedure does not significantly compromise the intrinsic electronic property of the nanotubes. A phospholipid and a protein were used for the surface modification of the nanotubes. A microchip was fabricated from the polymer nanocomposite and temperature distribution in a microchannel was investigated under NIR irradiation. Temperature control of an aqueous solution in the microchannel has been achieved, which makes this hybrid system suitable for various lab-on-a-chip applications.

Czanikova et al. developed photoactuating materials based on elastomers and modified CNTs [158]. The matrix of ethylene–vinylacetate was integrated with multi-walled CNTs. The nanotubes were surface functionalized with a pyrene cholesterol conjugate by the noncovalent approach to enhance its compatibility

and dispersibility in the elastomer matrix. Nanotubes were uniaxially aligned in the composite by shearing forces. The photoactuation behavior of the soft and responsive nanocomposites was investigated by atomic force microscopy and nanoindentation techniques. Czanikova et al. have also reported single-walled CNT-based photoactuators in ethylene vinyl acetate copolymer [159]. Photoactuation and relaxation behaviors of the nanocomposites with aligned nanotubes were studied with respect to CNT concentration, light intensity, etc.

Tang et al. reported CNT-dispersed poly(ethyleneglycol) (PEG) composites for solar energy conversion and storage [160]. They prepared a ternary nanocomposite using multi-walled CNT, PEG, and silicon dioxide. The composite could absorb sunlight and efficiently convert it into thermal energy and can act as an energy storage system. Given the huge demand for energy conversion and storage devices and systems, this simple ternary nanocomposite containing a photothermal agent and a phase change material is very interesting for fundamental studies and technological applications. Ilcikova et al. developed acrylic thermoplastic elastomers that were dispersed with block-copolymer-grafted CNTs [161]. The nanocomposite of the triblock copolymer containing diblock-copolymer-grafted CNTs exhibited photoactuating behavior. Under red light exposure, the elastomeric nanocomposite showed fast and reversible actuation. CNTs and fullerene-based hybrid systems have been developed and applied as temperature indicators by taking advantage of the photothermal conversion characteristic of CNTs [162]. CNTs and GNPs have also been employed as photothermal agent in the shape, morphology, and wetting properties of fullerene-based microparticles [163].

Graphene, the two-dimensional (2D) allotrope of carbon, has gained enormous attention [164]. Impressive electronic, optical, and mechanical properties along with high surface area have rendered graphene an appealing material. Insertion of graphene into polymer matrices has yielded significantly improved physical properties.

Liang et al. fabricated graphene-based nanocomposites that could be triggered by IR light and can act as actuators [165]. They dispersed sulfonated functionalized graphene particles into thermoplastic polyurethane to prepare light-driven nanocomposite actuators. The nanocomposite not only exhibited excellent photoactuation but also helped in significantly improving the mechanical properties of the hybrid system. Upon irradiation with IR light the nanocomposite undergoes contraction and thereby could lift a 21.6 g weight by 3.1 cm with a force of 0.21 N. The mechanical properties of the nanocomposites were found to improve with increase in graphene loading in the system. Comparison of different kinds of graphene materials has revealed that the light-driven actuation behavior of the nanocomposites depends on the nature of the aromatic network of graphene as well as the homogeneity of its dispersion in the matrix. Loomis et al. have revealed layer-dependent mechanical responses of graphene composites to NIR light [166]. They fabricated graphene nanosheet dispersed polymer nanocomposites and prepared thin films from the hybrid system. Nanocomposites containing single layer graphene and multilayer graphene were made for comparison of their physical response to NIR light irradiation. Both elastic moduli and stress response of the single layer and multilayer graphene containing composites were observed to be different from one another. The difference in behavior of these

composites has been attributed to the number of graphene layers in contact with the host polymer in the matrix. Loomis et al. have developed photothermal nanopositioners from graphene–elastomer nanocomposites [167]. The nanopositioners were fabricated from the nanocomposites made by dispersing graphene nanoplatelets into the soft and responsive matrix of PDMS. Upon light irradiation the grahene nanoplatelets absorb the photons and convert them into heat, thereby increasing the local temperature in the nanocomposite. They developed a two-axis stage with sub-micron resolution, which permitted two-axis positioning (120 nm resolution and about 5 μm s^{-1} speed) driven by photothermal effect. Good actuation speed and appreciable actuator efficiency were obtained for the nanocomposites. However, there is still room for improvement in the performance of the photothermal nanopositioners.

Ansari et al. made optical actuators from graphene and triblock copolymer composites [168]. Freestanding thin films were prepared from the nanocomposites containing graphene platelets in the matrix of the block copolymer poly(styrene-b-isoprene-b-styrene). Solvent casting technique was used in the preparation of the freestanding nanocomposite films. It was found that under strained conditions the nanocomposite film contracts upon IR irradiation. However, under stress-free conditions the films were found to expand. Such films could find application in biomedical field in situations where remote-controlled actuation is preferred. Meng et al. observed enhanced photothermal effect of graphene conjugated polymer composites [169]. Poly(3-hexylthiophene)-conjugated polymer was covalently grafted onto reduced graphene oxide sheets to prepare the hybrid system. This hybrid system exhibited superior photothermal effect when compared with the system without covalent linking. This enhanced performance has been attributed to photoinduced energy transfer from the conjugated polymer backbone to the reduced graphene oxide surface. Using a thin layer of this hybrid material a photocontrolled electrical switch has been demonstrated.

Muralidharan et al. prepare nanocomposites from biocompatible natural polymer chitosan and reduced graphene oxide [170]. Using solvent casting technique they obtained nanocomposite-based actuators that exhibit photomechanical actuation under IR light illumination. The samples studied underwent contraction in length in response to IR exposure. Light-induced stress and strain were found to increase upon increase in reduced graphene oxide loading in the actuator matrices. In this system the applied pre-strain was found to reduce photomechanical stress of the actuators, which is an unusual behavior. Since photomechanical actuation in the nanocomposite is dependent on the concentration of graphene oxide and the applied pre-strain, the actuation behavior could be tuned by varying these two parameters. Leeladhar et al. demonstrated the fabrication of highly versatile photomechanical actuators using graphene platelets dispersed in PDMS matrix [171]. The actuators were prepared in a bilayer actuator where a thin layer of chromium was coated on one side of the polymer nanocomposite film. The bilayer actuators were found to exhibit fast and reversible actuation with a large deflection angle. Moreover, the actuator was found to exhibit photoresponse depending on the wavelength used. The large bending observed has been ascribed to the mismatch of the coefficients of thermal expansion between the two layers.

Robinson et al. developed biocompatible reduced-graphene-oxide-based hybrid materials that exhibit high absorption in the NIR region [172]. Single-layered reduced graphene oxide nanosheets were noncovalently surface functionalized with amphiphilic PEGylated polymer chains, which are able to show sixfold higher NIR absorption when compared to their nonreduced and covalently functionalized counterparts. Photoablation of U87MG cancer cells was demonstrated *in vitro* by employing reduced graphene oxide hybrids bearing a peptide with the Arg–Gly–Asp (RGD) moiety as photothermal agents. The reduced graphene oxide hybrid system, which is biocompatible and exhibits high NIR absorption, could be useful for photothermal therapy of cancer.

Feng et al. prepared polyurethane-based efficient actuators by incorporating functionalized reduced graphene oxide and CNTs into the polymer matrix [173]. These polyurethane hybrids containing the nanofillers exhibit good IR light absorption and consequent actuation. By adjusting the doping ratio of reduced graphene oxide and CNT, impressive IR-actuated stress recovery has been achieved in these multicomponent photothermal systems. Niu et al. have demonstrated a photomechanical soft actuator that has been fabricated from PDMS doped with graphene nanoplatelets [174]. The soft actuator is made up of a bilayer film: one layer is the graphene-dispersed PDMS and the other layer is pure PDMS. In this bilayer system, the mismatch between the coefficients of thermal expansion of the layers has been utilized to achieve controllable and reversible bending in response to NIR light irradiation. Different bending behavior has been registered by selecting the layer for exposure to light source. The occurrence of temperature gradient across the thickness of the layers has been assumed to be responsible for the distinct bending behavior observed.

Organic conjugated polymers capable of conducting ions and electrons have been developed and extensively investigated. Their applications in organic electronic and optoelectronic devices such as solar cells, field effect transistors, and light-emitting diodes have been well documented. Apart from these well-known applications, their suitability in various other areas has been assessed and they have been employed in high-tech applications such as biomedical science, biosensing, supercapacitor, chemical sensing, and fluorescence imaging. Owing to their extended conjugation length, many conducting polymers could absorb IR radiation and through nonradiative relaxation can produce heat. This energy transduction property of the conjugated polymers qualifies them as an attractive class of organic photothermal agents. Consequently, they have been used in both *in vitro* and *in vivo* photothermal therapy of cancer. These polymers could also be used as highly efficient drug delivery systems with large loading capacity. Thus, they could be useful in combination therapies. Recently conjugated polymers with large absorption coefficient, good photostability, bicompatibility, biodegradability, and acceptable photothermal conversion efficiencies have been realized and their application potential as photothermal agents has been evaluated.

Yang et al. reported organic nanoparticles based on the conducting polymer polyaniline and used them as photothermal agents in the ablation of cancer cells by light irradiation [175]. Polyaniline can exist in emeraldine base (EB) or emeraldine salt (ES) state. The EB form of polyaniline can be readily converted into the ES state by doping process (Figure 1.14). The doping process shifts the

Figure 1.14 Schematic illustration of the preparation of organic photothermal agents based on polyaniline nanoparticles and their application for the photothermal ablation of epithelial cancer cells by NIR laser irradiation. Source: Yang et al. 2011 [175]. Copyright 2011. Reproduced with permission from Wiley-VCH Verlag GmbH & Co. KGaA.

absorption of polyaniline into the NIR region of the electromagnetic spectrum by decreasing the energy bandgap. Polyaniline is found to be capable of converting the absorbed NIR light into heat and is biocompatible. Therefore, it has been used as an organic photothermal agent in photothermal therapy of cancer. Water soluble and stable polyaniline nanoparticles have been prepared by nanoemulsion method and have been applied in the treatment of epithelial cancer cells using NIR light. Similar surface-coated polyaniline nanoparticles have also been used for both *in vitro* and *in vivo* photothermal therapy of cancer [176]. The surface-functionalized uniform polyaniline nanoparticles were found to possess high extinction coefficient and exhibit higher photothermal conversion efficiency. Low toxicity of these photothermal nanoparticles to living cells has been ascertained using a variety of analytical characterization techniques.

Geng et al. designed and synthesized biocompatible conjugated polymer nanoparticles for efficient photothermal tumor therapy [177]. They have judiciously engineered the polymer backbone through the coupling of donor and acceptor moieties. Polymer nanoparticles were fabricated using a suitable precipitation method in an encapsulation matrix. Both *in vitro* and *in vivo* cancer cell killing by NIR light irradiation has been demonstrated using these polymer nanoparticles with large absorption coefficient. Such carefully designed polymers could find use in photothermal cancer therapy.

Lyu et al. developed and used the photothermal effect of semiconducting polymer bioconjugates for activation of targeted neurons [178]. The semiconducting bioconjugates have been found to possess higher photothermal conversion efficiency than GNRs. They have demonstrated NIR-light-driven control of thermosensitive ion channels in neurons using the polymer bioconjugates. Owing to the fast energy conversion ability to heat and high spatial precision to the ion channel, safe and reversible activation of the intracellular calcium ion influx of neuronal cells has been accomplished using the polymer bioconjugates. This method is benign in that it does not involve genetic transfection. This organic nanoparticle-based photothermal technique is powerful and could be a potential alternative to optogenetics. Lyu et al. have demonstrated *in vivo* photothermal therapy using semiconducting polymer nanoparticles [179]. They carried out intraparticle molecular orbital manipulation to enhance the photothermal efficiency of the polymer nanoparticles for cancer therapy. For this purpose, they have used fullerene particles in combination with semiconducting polymers. The energy levels of the donor polymer and acceptor fullerene derivative have been so aligned that photoinduced electron transfer occurs efficiently and quenches the fluorescence in the system. This leads to nonradiative relaxation following light irradiation and thus produces heat. This approach to photothermal therapy could be extended to other binary composite systems. Cao et al. designed and synthesized an organic conjugated polymer and found that it possessed high efficiency in photothermal conversion [180]. The conjugated polymer prepared contains donor and acceptor entities in its structure and has a very narrow bandgap. The narrow bandgap enables the polymer to absorb NIR light. This photostable polymer with high extinction coefficient exhibits high photothermal conversion. The photothermal effect of the polymer has been used to drive temperature-dependent devices. The conjugated polymer could be applicable in

biomedical technology due to its high absorbance in the biocompatible NIR window.

1.4 Gels Driven by Photothermal Effect

Gels are a promising class of soft materials. They have been extensively investigated in materials science and bioscience owing to their outstanding characteristics and a variety of potential and practical applications [181–185]. Gels do not flow and exhibit solid-like rheology. Stimuli responsiveness, adaptability, and self-healing of morphological defects are some of their excellent attributes. Gels contain a large volume of liquid (water or organic solvent), which is immobilized by a network of gelators. The gelators could be small molecules with low molecular weight or macromolecules with high molar mass. Hydrogels are made up of water as the solvent whereas organogels contain organic solvents. Gels can vary in the nature of network formation by the gelators. The gelators can form chemically cross-linked networks via covalent bonding or exhibit physically cross-linked networks through noncovalent supramolecular interactions. Different properties are observed in different types of gels. It should be noted that gels can also be fabricated from LC phases using suitable gelators. Unlike in hydrogels and organogels, the solvent in LC gels is an anisotropic fluid medium. Advanced nanocomposites have been developed by dispersing nanoscale particles into the matrix of gels. Nanocomposites of gels could exhibit superior properties than the pure host gels due to the synergy between complementary strengths of the two functional components in one system. Recently, distinct nanocomposite gels containing different photothermal agents have been attracting considerable amount of attention. Application prospects of such nanocomposites have been demonstrated in materials science, biomedical science, optomechanics, microfluidics, drug delivery, etc. Moreover, the gel nanocomposites are interesting hybrid systems to understand how collective properties arise from interaction between the components within the soft stimuli-responsive matrices.

Mebrouk et al. have designed and synthesized nickel bis(dithiolene)-based gelators containing pendant cholesteryl moieties [186]. They have fabricated gels using these metal complexes that form intertwined fibers. It was observed that the nickel bis(dithiolene) derivatives exhibit efficient absorption of NIR light comparable to GNPs and convert it into heat in the gel matrix. Taking advantage of this photothermal property, the stability of the gels could be modulated by NIR light irradiation. Such photothermal gels could offer new opportunities in materials science and nanotechnology owing to the facile realization of photothermal gelators.

Wang et al. have developed an injectable hydrogel that can be used to carry out photothermal therapy of cancer [187]. Interestingly, the hydrogel could be degraded on demand following therapy to clear out from the body, thereby reducing the risk of cytotoxicity that arises due to long-term retention of hydrogel in the body. The hydrogel is based on alginate-calcium, which immobilizes platinum nanoparticles containing dendrimers (Figure 1.15). The hydrogel is biocompatible and degrades upon injection of appropriate chelates. Here the
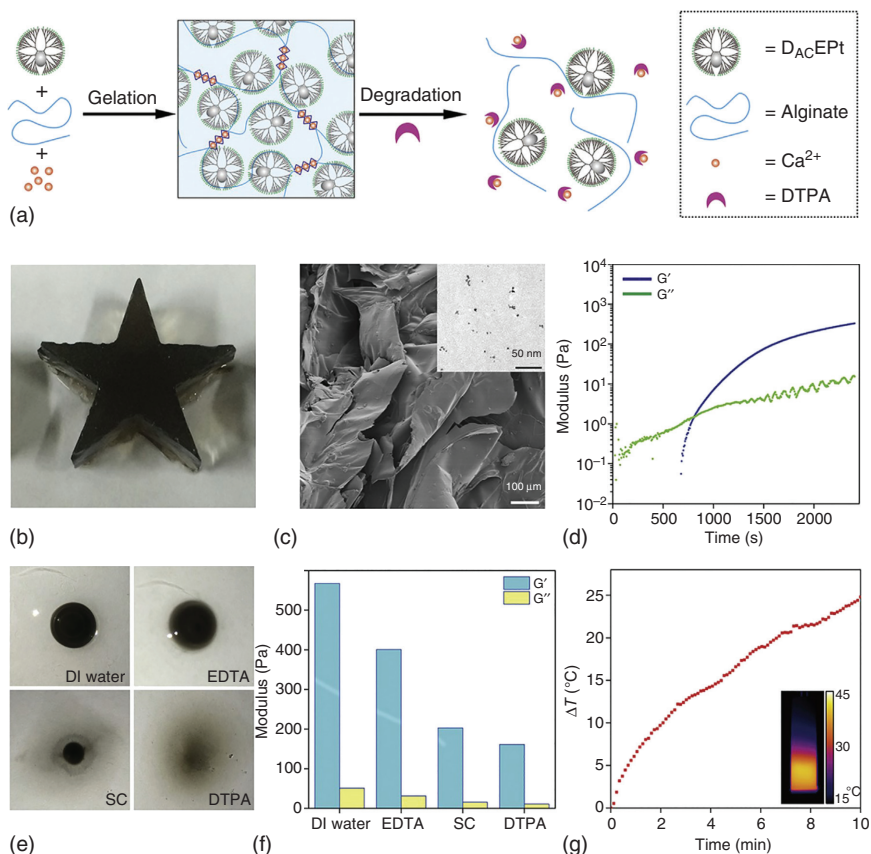
Figure 1.15 Schematic depicts the gelation and on-demand degradation of the gel.
Source: Wang et al. 2016 [187]. Copyright 2016. Reproduced with permission from Elsevier.

dendrimer-encapsulated platinum nanoparticles act as photothermal centers and raise the surrounding temperature upon NIR irradiation. It has been observed that this hydrogel could ablate tumors when coated onto the tumor instead of being injected into it. This protocol of injection and on-demand degradation of the hydrogel in cancer photothermal therapy is attractive since it not only reduces the adverse effects but also drastically diminishes toxicity in the body.

Zheng et al. developed supramolecular hydrogels that are capable of exhibiting switchable size and dynamic mechanical properties in response to light of different wavelengths (Figure 1.16) [188]. The gel containing dendrimer-encapsulated platinum nanoparticles displays softening and stiffening in response to UV and NIR light irradiation. The gel is found to shrink in size upon NIR light irradiation; however, it recovers when the NIR source is put off. A photothermally driven high-strength double-network gel has been developed, which exhibits IR-light-induced actuation behavior [189].

Mohamed et al. have investigated the dynamics of hot electrons and phonons of GNPs that are inserted in gel matrices and irradiated by laser pulses [190].
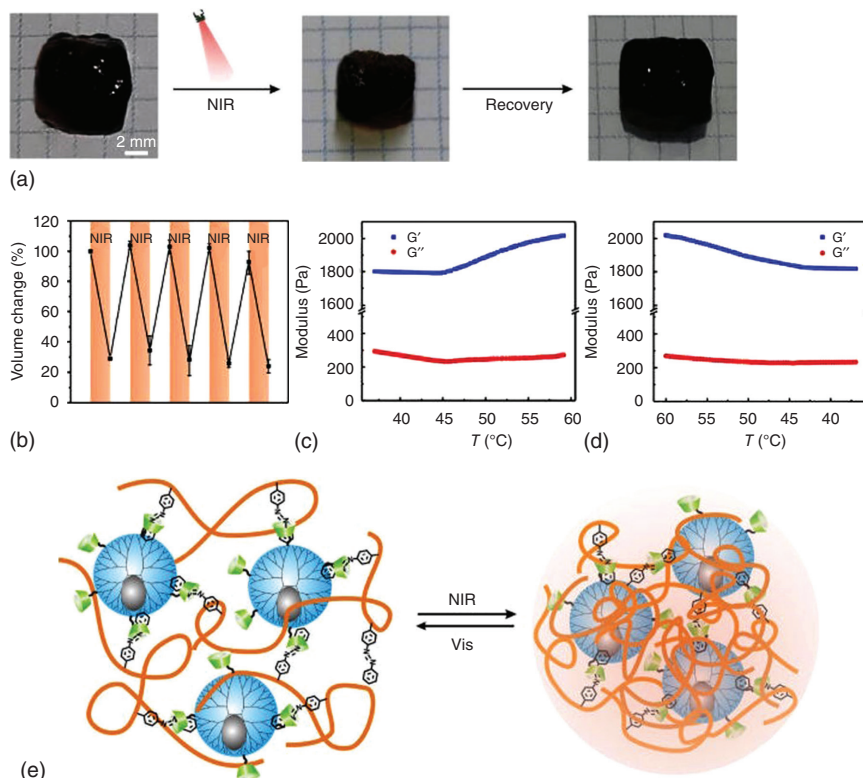
Figure 1.16 NIR-responsive behavior of the supramolecular gel. (a) Photographs of the supramolecular gel irradiated by an NIR laser. (b) Changes in the volume of the gel when an NIR laser is periodically turned on and off. (c, d) Stiffness of the gel at varying temperatures. (e) Mechanism of the NIR-responsive gel. Source: Zheng et al. 2017 [188]. Copyright 2017. Reproduced with permission from The American Chemical Society.

Electron–phonon and phonon–phonon coupling relaxation times have been found to increase in the hydrogel and organogel matrices compared to the aqueous solution. Kim and Lee have developed hydrogel-coated GNPs with different shell thicknesses [191]. Owing to the biocompatibility of the hydrogel polymer shell, these hybrid nanoparticles could serve as drug delivery vehicles. Moreover, the hydrogel shell of the nanoparticles could be easily thermally activated by exposure to light with wavelengths that fall in the plasmon absorption band of the GNP core. Kawano et al. designed and synthesized gel-coated GNRs [192]. These hybrid core–shell nanorods served as heating centers in targeted delivery in response to NIR laser irradiation. They show remote and reversible *in vivo* action upon NIR irradiation. These nanorods can be employed as probes for *in vivo* imaging techniques. *In vivo* fabrication of hydrogels needs delivery of two different solutions that would spontaneously cross-link upon mixing. However, in such processes the kinetics of gelation is difficult to control. To address this issue, Gramlich et al. carried out transdermal gelation using GNRs and NIR light irradiation [193]. The heat produced during NIR irradiation of the nanorods

brings about polymerization leading to gelation. The characteristics of gels thus produced could be modulated spatially and temporally by changing the experimental parameters. This method is a promising protocol toward gelation through tissue using light that could penetrate tissue without harmful effects.

Stowers et al. have demonstrated dynamic tuning of the stiffness of a 3D hydrogel by light irradiation [194]. Hydrogels are widely used to unravel the role of stiffness on cell behavior since cell phenotype is greatly affected by the stiffness of the extracellular matrix. However, in biological processes the change in matrix stiffness is dynamic. In this context, a hydrogel with tunable stiffness over time could serve as a model system. For this purpose, they developed a system where alginate gel stiffness can be temporally modulated. The stiffness modulation of the gel was carried out by light-triggered release of calcium or a chelate from liposomes (Figure 1.17). Both dynamic stiffening and softening have been demonstrated in the system. This method could be extended to transdermal stiffness modulation by IR light irradiation.

Collins et al. have investigated charge modulation of a GNR in an ion gel device [195]. GNRs were added into an ion gel capacitor and changes in the electron concentration were studied using dark-field imaging spectroscopy.

Park et al. have developed a drug delivery system based on micro-organogels and loaded with GNRs [196]. They prepared the micro-organogels by emulsification technique using gelator fiber and vegetable oil, which served as a biocompatible drug carrier. A nonsteroidal anti-inflammatory model drug was encapsulated into the micro-organogel matrix for evaluation of the drug delivery properties. The drug delivery system released the model drug slowly in the absence of NIR light irradiation. However, upon exposure to NIR light the drug release was significantly accelerated owing to temperature increase of the GNR-containing drug delivery system that transforms the gel into liquid (Figure 1.18). The micro-organogel nanocomposite has the potential for on-demand drug delivery applications.

Sershen et al. have demonstrated independent control of microfluidic valves using nanocomposite hydrogels containing GNPs [197]. The hydrogel has been formed by poly(N-isopropylacrylamide), which exhibits reversible thermal phase changes. Fluid flow through the valves can be controlled by adjusting the intensity of the light source. Shiotani et al. have observed light-driven fast shrinking of a polymer hydrogel that was loaded with GNRs [198]. A model drug-loaded composite was prepared from the hydrogel and it was observed that the system rapidly releases the drug upon NIR laser irradiation. Moreover, irradiation region-specific release of the drug has been demonstrated by taking advantage of the high spatial resolution of light irradiation of the nanocomposite gel. Erdogan et al. have shown light-triggered control of degelation in peptide-based organogels embedded with GNPs [199]. They have used GNPs of different sizes and different shapes to evaluate their degelation capability under light irradiation. The control over degelation of biological molecules could offer promising possibilities in nanomedicine, drug delivery, nanodiagnostics, and tissue engineering. Zhou et al. have fabricated photothermally responsive hydrogel nanocomposites and developed micropatterned bilayer photoactuators that exhibit rapid and reversible bending and unbending movements upon
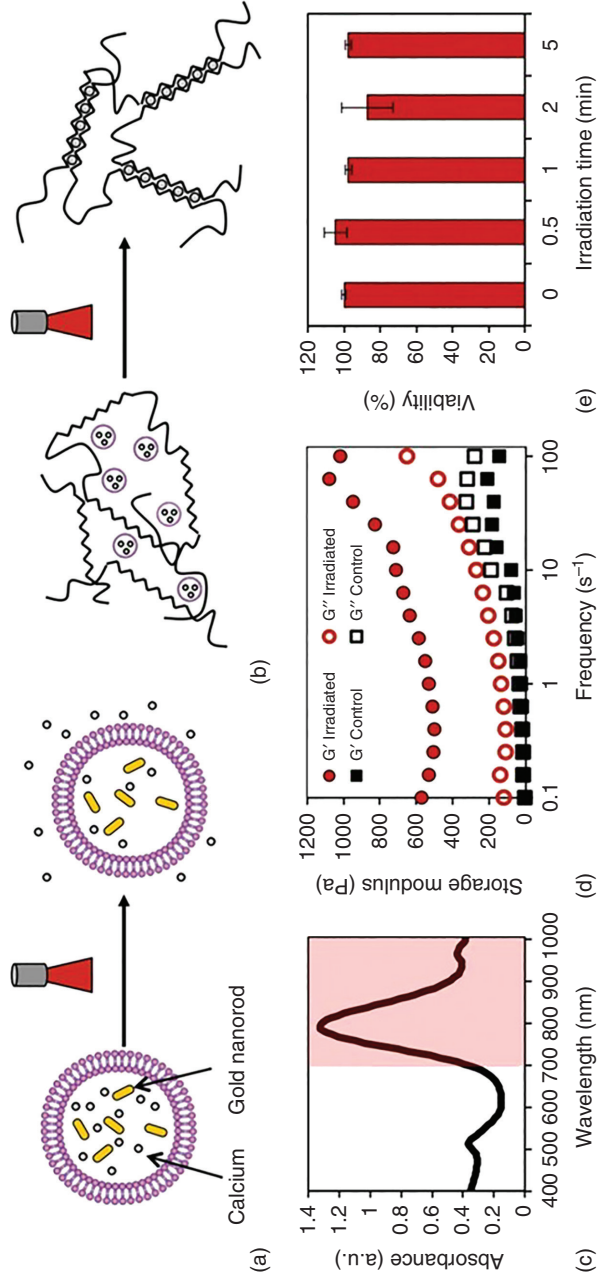
Figure 1.17 Mechanism of light-triggered release from liposomes. (a) Schematic of temperature-sensitive liposome loaded with gold nanorods and calcium. Upon irradiation, gold nanorods heat the lipid bilayer past its transition temperature, allowing calcium to permeate the lipid bilayer. (b) Irradiation of liposomes mixed with an alginate solution causes release of calcium and an increase in cross-linking density. (c) Absorbance spectrum of gold nanorods, demonstrating the narrow peak in NIR region. Shading denotes the optical window of highest penetration depth through tissue. (d) Rheometry of alginate: liposome solutions after irradiation. Irradiation causes release of calcium and gelation, shown by increased G' over controls. (e) MTS assay demonstrates no loss of viability after irradiation of cell-seeded gels. Source: Stower et al. 2015 [194]. Copyright 2015. Reproduced with permission from National Academy of Sciences.
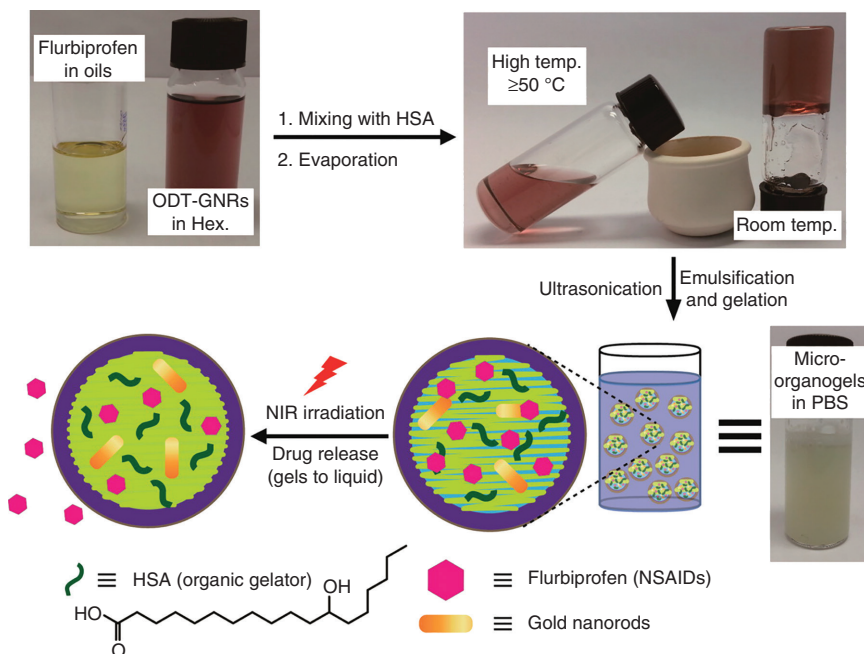
Figure 1.18 Schematic illustration for formation of GNR-containing micro-organogels and their drug release upon NIR irradiation. Source: Park et al. 2016 [196]. Copyright 2016. Reproduced with permission from The American Chemical Society.

exposure to visible light [200]. Light-waveguided through optical fiber directly into the photoactuator film has been found to be equally effective in causing actuation as free space light.

Lo et al. have developed a new light-responsive poly(*N*-isopropylacrylamide) hydrogel nanocomposite incorporating glycidyl-methacrylate-functionalized graphene oxide [201]. The hydrogel nanocomposites were produced using photopolymerization technique. The highly efficient photothermal conversion of glycidyl methacrylate-functionalized graphene oxide was found to cause large volume change of the nanocomposite hydrogels upon exposure to IR light. This large volume change has been exploited in the fabrication and operation of a microvalve that is able to control fluidic flow in the channel by remote actuation with IR light. Zhang et al. have fabricated CNT-containing hydrogel polymer composites and investigated their responsive behavior [202]. The polymer hydrogel was obtained using poly(*N*-isopropylacrylamide). Polymer hydrogel nanocomposites were fabricated by dispersing single-walled CNTs into the soft hydrogel matrix. Fast photomechanical actuation was observed in the hydrogel nanocomposites upon exposure to NIR light due to strong absorption by the CNTs. The response time of the actuators could be tuned by varying the loading level of CNTs in the matrix. Cubes and flowers capable of self-folding have been demonstrated using the polymer hydrogel nanocomposites. Zhang et al. fabricated graphene-oxide-containing polymer hydrogel nanocomposites capable of IR-light-driven actuation [203]. They have prepared a bilayer architecture using

graphene-oxide-containing hydrogel and another hydrogel without graphene oxide. Upon IR irradiation the bilayer undergoes anisotropic bending motion due to the temperature increase in the hydrogel layer containing graphene oxide particles.

Zhu et al. synthesized a hydrogel nanocomposite containing graphene oxide and investigated its photothermal responsiveness [204]. The hydrogel was synthesized by *in situ* polymerization of *N*-isopropylacrylamide monomers in an aqueous solution dispersed with graphene oxide. The gel exhibits reversible phase transition upon irradiation with NIR laser. They have demonstrated the application potential of the nanocomposite gel in a microfluidic device for controlled fluid flow (Figure 1.19a–d). Such gels with superior photothermal sensitivity could find application in biomaterials and biomedical devices.

Fujigaya et al. have studied reversible volume change in CNT-containing gels upon NIR light irradiation [206]. These nanocomposite gels were found to possess excellent fatigue resistance during ON/OFF cycles. Li et al. have developed hydrogel nanocomposites by incorporating graphene oxide into a polymer matrix [207]. The hydrogels can be facilely triggered by NIR light irradiation. Using these functional gels as 3D scaffolds they demonstrated reversible cell capture and on-demand release by light exposure. Wang et al. have developed light-driven hydrogel actuators from genetically engineered elastin-like polypeptides doped with reduced graphene oxide particles [208]. Tunable motions with spatial resolution such as finger-like flexing as well as crawling has been demonstrated in these hybrid systems that can be controlled by varying different parameters of light source. Cong et al. have demonstrated water treatment using a thermoresponsive nanocomposite hydrogel containing graphene particles [209]. These mechanically robust hydrogel composites exhibited high adsorption capacity and good recyclability in treating water. Reduced-graphene-oxide-dispersed hydrogel composites have been used for the fabrication of bendable bilayer-type photoactuators that can be driven by visible light irradiation [210].

Satarkar et al. have reported the fabrication and investigation of remote-controlled microfluidic valves using magnetic nanoparticle hydrogels [211]. Gallium-based liquid metal alloys are recently attracting considerable attention in microfluidic devices as functional fluid microcomponents such as valves, heaters, and electrodes [212, 213]. Local switching of chemical patterns has been achieved by Yoon et al. employing the creased surface of a hydrogel [214]. The hydrogel was impregnated with iron oxide nanoparticles, which exhibit photothermal effect. Upon exposure to light the hydrogel temperature rises due to the photothermal conversion by the iron oxide nanoparticles, which causes volume change in the system. Light-controlled microvalves have been developed by Lee et al. using hydrogels incorporated with photothermal iron oxide nanoparticles [215]. For this purpose, they prepared the hydrogel composite that is capable of fast response and substantial volume change upon exposure to light. Movable position heating source [216], photoactuators from comb-type hydrogels [217], and stimuli-responsive hydrogel microfibers [218] have been obtained using photothermal magnetic nanoparticles dispersed into hydrogel matrices.

Hsiao et al. have used *in situ* formed NIR-absorbing micellar hydrogels in photothermal tumor ablation [205]. They have designed and synthesized a

chitosan derivative functionalized with conjugated polymer polyaniline as side chains. This covalently linked hybrid polymer material is able to self-assemble into micelles. The micelles could be transformed into hydrogels by appropriately adjusting the pH of the micellar solution. Owing to the presence of the conducting polymer polyaniline in its structure, the micelles are able to absorb NIR light and convert it into heat. This photothermal property of the micelles was used in the selective destruction of cancer cells in light-exposed areas. The efficiency of the micellar hydrogel in photothermal therapy has been evaluated using a tumor-bearing mouse model (Figure 1.19e). This model study demonstrated
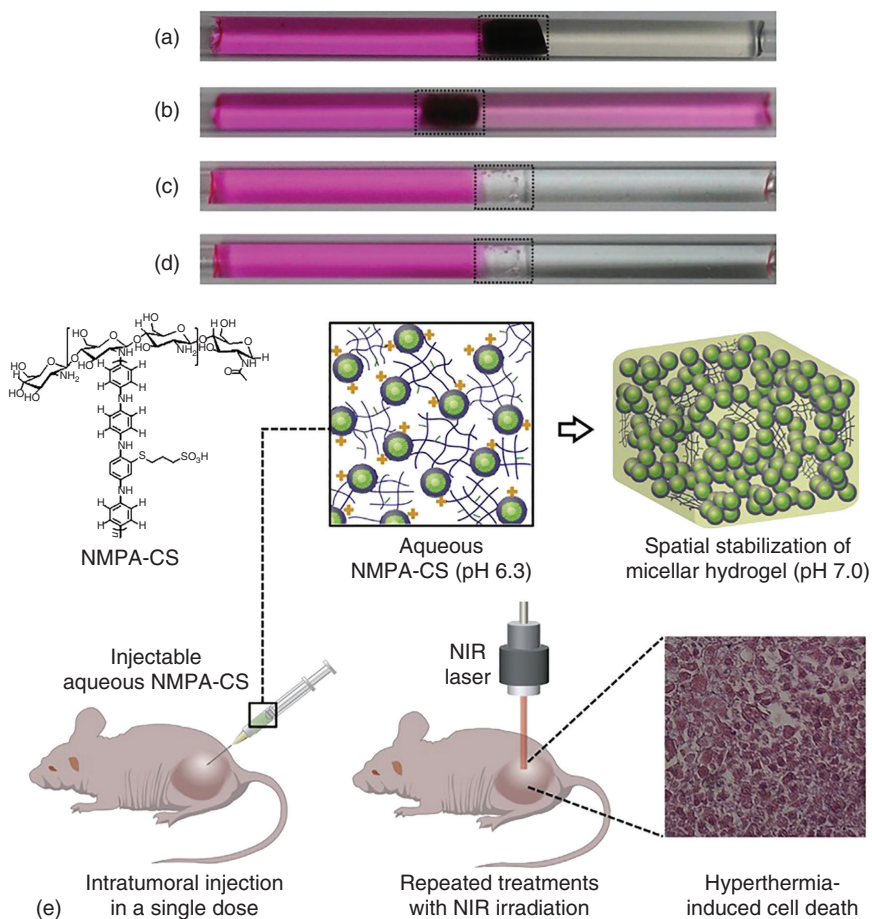
Figure 1.19 (a–d) Liquid microvalves made with the PNIPAM/GO hydrogel (a, b) and a PNIPAM hydrogel (c, d). The photographs show the microvalves before (a, c), after (b, d) NIR (808 nm, 2 W) irradiation for two minutes, where the positions of the hydrogels are marked by the rectangular boxes. The solutions encapsulated in the left and right sides are a red rhodamine solution and light yellow NiSO$_4$, respectively. Source: Gramlich et al. 2014 [193]. Copyright 2012. Reproduced with permission from Wiley-VCH Verlag GmbH & Co. KGaA. (e) Chemical structure of CS derivative that contained self-doped PANI side-chains and mechanism by which it photothermally treats tumors. Source: Hsiao et al. 2016 [205]. Copyright 2015. Reproduced with permission from Elsevier.

that biocompatible NIR-absorbing micellar hydrogels can be formed in the target site for minimal invasive photothermal treatment of cancer.

1.5   Summary and Outlook

The combination of soft materials and photothermal agents is emerging as an enabling endeavor. Functional soft composite materials fabricated by bringing these two classes of interesting materials have been demonstrated to act as actuators, therapeutic agents, drug delivery systems, microvalves, etc. Remotely triggered photoinduced phase transitions have been carried out by taking advantage of the photothermal effects of the photothermal agents. Inorganic metal (gold, platinum) nanoparticles, iron oxide nanoparticles, carbon nanomaterials (CNTs, graphene derivatives), and organic compounds (small molecule dyes and conducting polymers) have been employed as photothermal agents to drive LCs, polymers, and gels. The photothermal effect of GNPs has been used in drug delivery application of lyotropic LCs and they have enabled optical property modulation of self-assembled thermotropic 1D and 3D photonic crystals. Light-driven dynamic shape morphing and photomechanical actuations such as bending, twisting, folding, and oscillations have been achieved by combining photothermal agents with functional polymers and elastomers. Photothermally activated hydrogels have been employed in efficient water treatment and control of fluid flow in microfluidic devices. Smart and adaptive systems have been realized by dispersing photothermal agents into soft matter matrices. Synergy between the properties of soft materials and photothermal agents has been found to enhance the functionalities of the stimuli-responsive composites. In addition to physical mixing of photothermal agents with the soft matrices, they have also been covalently conjugated in the systems to fabricate better performing and robust materials. In many instances, the photothermal agents have been suitably functionalized to enhance their compatibility and homogeneous dispersion in the host matrices, thereby increasing their efficiency. However, phase separation at higher loading amounts remains an issue with the photothermal agents, which requires a great deal of attention. In drug delivery and photothermal therapy the long-term toxicity of the agents needs to be systematically evaluated before they could be clinically viable. Inorganic nanoparticles, being nondegradable, could accumulate in the cell and cause toxicity if they are not efficiently cleared from the body after they have performed their job. To address this issue, appropriate physical and chemical functionalization of inorganic nanoparticles is being developed and assessed. However, it needs extensive evaluation by materials scientists and clinicians for commercial applications. Organic photothermal agents have certain advantages over their inorganic counterparts; however, it is necessary to make a different variety of organic agents available for use. The covalent linking of conjugated polymers and NIR-absorbing dyes with soft matter components seems to be a promising approach to take advantage of the photothermal effect of organic agents; nevertheless, robust and versatile functionalization protocols that are facile and benign need to be developed and optimized to exploit the full potential of organic photothermal agents. The work accomplished in

driving soft materials by photothermal effect and the applications demonstrated have laid the groundwork for further exploration. This area of research is in its early infancy and it is expected to make great strides in materials science, nanotechnology, bioscience, and beyond with the availability of appropriately engineered materials and processing techniques.

Acknowledgments

References

1 de Gennes, P.-G. (1992). Soft matter. *Angew. Chem. Int. Ed. Engl.* 31: 842.
2 de Gennes, P.-G. (1992). Soft matter. *Rev. Mod. Phys.* 64: 645.
3 Hamley, I.W. (2007). *Introduction to Soft Matter: Synthetic and Biological Self-Assembling Materials*. Chichester, UK: Wiley.
4 Li, Q. (ed.) (2013). *Intelligent Stimuli Responsive Materials: From Well-defined Nanostructures to Applications*. Hoboken, NJ: Wiley.
5 Kleman, M. and Lavrentovich, O.D. (2003). *Soft Matter Physics: An Introduction*. New York: Springer-Verlag.
6 Selinger, J.V. (2016). *Introduction to the Theory of Soft Matter: From Ideal Gases to Liquid Crystals*. New York: Springer-Verlag.
7 Hirst, L.S. (2012). *Fundamentals of Soft Matter Science*. Boca Raton, FL: CRC Press.
8 Mezzenga, R., Schurtenberger, P., Burbidge, A., and Michel, M. (2005). Understanding foods as soft materials. *Nat. Mater.* 4: 729.
9 Marchetti, M.C., Joanny, J.F., Ramaswamy, S. et al. (2013). Hydrodynamics of soft active matter. *Rev. Mod. Phys.* 85: 1143.
10 Nagel, S.R. (2017). Experimental soft-matter science. *Rev. Mod. Phys.* 89: 025002.
11 Wang, L. and Li, Q. (2016). Stimuli-directing self-organized 3D liquid crystalline nanostructures: from materials design to photonic applications. *Adv. Funct. Mater.* 26: 10.
12 Bisoyi, H.K., Bunning, T.J., and Li, Q. (2018). Stimuli-driven control of the helical axis of self-organized soft helical superstructures. *Adv. Mater.* 30: 1706512.
13 Bisoyi, H.K. and Li, Q. (2016). Light-directed handedness inversion of self-organized helical superstructure: dynamic photoswitching the chirality of circularly polarized reflection. *Angew. Chem. Int. Ed.* 55: 2994.
14 Hamley, I.W. (2003). Nanotechnology with soft materials. *Angew. Chem. Int. Ed.* 42: 1692.

15 Quake, S.R. and Scherer, A. (2000). From micro- to nanofabrication with soft materials. *Science* 290: 1536.

16 Rogers, J.A. and Nuzzo, R.G. (2005). Recent progress in soft lithography. *Mater. Today* 8: 50.

17 Whitesides, G.M. and Lipomi, D.J. (2009). Soft nanotechnology: "structures" vs. "function". *Faraday Discuss.* 143: 373.

18 Whitesides, G.M. (2018). Soft robotics. *Angew. Chem. Int. Ed.* 57: 4258.

19 Li, Q. (ed.) (2018). *Functional Organic and Hybrid Nanostructured Materials: Fabrication, Properties, and Applications*. Weinheim: Wiley-VCH.

20 Wang, L. and Li, Q. (2018). Photochromism into nanosystems: towards lighting up the future nanoworld. *Chem. Soc. Rev.* 47: 1044.

21 Bisoyi, H.K. and Li, Q. (2014). Light-directing chiral liquid crystal nanostructures: from 1D to 3D. *Acc. Chem. Res.* 47: 3184.

22 Wang, Y. and Li, Q. (2012). Light-driven chiral molecular switches or motors in liquid crystals. *Adv. Mater.* 24: 1926.

23 Qin, Z. and Bischof, J.C. (2012). Thermophysical and biological responses of gold nanoparticle laser heating. *Chem. Soc. Rev.* 41: 1191.

24 Abadeer, N.S. and Murphy, C.J. (2017). Recent progress in cancer thermal therapy using gold nanoparticles. *J. Phys. Chem. C* 120: 4691.

25 Riley, R.S. and Day, E.S. (2017). Gold nanoparticle-mediated photothermal therapy: applications and opportunities for multimodal cancer treatment. *WIREs Nanomed. Nanobiotechnol.* 9: e1449. doi: 10.1002/wnan.1449.

26 Song, X., Chen, Q., and Liu, Z. (2015). Recent advances in the development of organic photothermal nano-agents. *Nano Res.* 8: 340.

27 Bao, Z., Liu, X., Liu, Y. et al. (2016). Near-infrared light-responsive inorganic nanomaterials for photothermal therapy. *Asian J. Pharm. Sci.* 11: 349.

28 Shi, C., Wu, J.B., and Pan, D. (2016). Review on near-infrared heptamethine cyanine dyes as theranostic agents for tumor imaging, targeting, and photodynamic therapy. *J. Biomed. Opt.* 21: 050901.

29 Huang, X., Jain, P.K., El-Sayed, I.H., and El-Sayed, M.A. (2008). Plasmonic photothermal therapy (PPTT) using gold nanoparticles. *Lasers Med. Sci.* 23: 217.

30 Yuan, A., Wu, J., Tang, X. et al. (2013). Application of near-infrared dyes for tumor imaging, photothermal and photodynamic therapies. *J. Pharm. Sci.* 102: 6.

31 Melamed, J.R., Edelstein, R.S., and Day, E.S. (2015). Elucidating the fundamental mechanisms of cell death triggered by photothermal therapy. *ACS Nano* 9: 6.

32 Huang, X. and El-Sayed, M.A. (2011). Plasmonic photo-thermal therapy (PPTT). *Alexandria J. Med.* 47: 1.

33 Wang, J. and Quiz, J. (2016). A review of organic nanomaterials in photothermal cancer therapy. *Cancer Res. Front.* 2: 67.

34 Huang, X., Zhang, W., Guan, G. et al. (2017). Design and functionalization of the NIR-responsive photothermal semiconductor nanomaterials for cancer theranostics. *Acc. Chem. Res.* 50: 2529.

35 Yang, K., Feng, L., Shi, X., and Liu, Z. (2013). Nano-graphene in biomedicine: theranostic applications. *Chem. Soc. Rev.* 42: 530.

36 Qiu, J. and Wei, W.D. (2014). Surface plasmon-mediated photothermal chemistry. *J. Phys. Chem. C* 118: 20735.

37 Fablan, J., Nakazumi, H., and Matsuoka, M. (1992). Near-infrared absorbing dyes. *Chem. Rev.* 92: 1197.

38 Qian, G. and Wang, Z.Y. (2010). Near-infrared organic compounds and emerging applications. *Chem. Asian J.* 5: 1006.

39 Xu, L., Cheng, L., Wang, C. et al. (2014). Conjugated polymers for photothermal therapy of cancer. *Polym. Chem.* 5: 1573.

40 Webb, J.A. and Bardhan, R. (2014). Emerging advances in nanomedicine with engineered gold nanostructures. *Nanoscale* 6: 2502.

41 Her, S., Jaffray, D.A., and Allen, C. (2017). Gold nanoparticles for applications in cancer radiotherapy: mechanisms and recent advancements. *Adv. Drug Delivery Rev.* 109: 84.

42 Jaque, D., Maestro, L.M., del Rosal, B. et al. (2014). Nanoparticles for photothermal therapies. *Nanoscale* 6: 9494.

43 Hu, Y., Li, Z., Lan, T., and Chen, W. (2016). Photoactuators for direct optical-to-mechanical energy conversion: from nanocomponent assembly to macroscopic deformation. *Adv. Mater.* 28: 10548.

44 Zhang, A., Li, A., Zhao, W., and Liu, J. (2018). Recent advances in functional polymer decorated two-dimensional transition-metal dichalcogenides nanomaterials for chemo-photothermal therapy. *Chem. Eur. J.* 24: 4215.

45 Dou, L., Liu, Y., Hong, Z. et al. (2015). Low-bandgap near-IR conjugated polymers/molecules for organic electronics. *Chem. Rev.* 115: 12633.

46 Cheng, L., Wang, C., Feng, L. et al. (2014). Functional nanomaterials for phototherapies of cancer. *Chem. Rev.* 114: 10869.

47 Jain, P.K., Huang, X., El-Sayed, I.H., and El-Sayed, M.A. (2008). Noble metals on the nanoscale: optical and photothermal properties and some applications in imaging, sensing, biology and medicine. *Acc. Chem. Res.* 41: 1578.

48 Watts, C.M., Liu, X., and Padilla, W.J. (2012). Metamaterial electromagnetic wave absorbers. *Adv. Mater.* 24: OP98–OP120.

49 Bayazitoglu, Y., Khedarmand, S., and Tullius, T.K. (2013). An overview of nanoparticle assisted laser therapy. *Int. J. Heat Mass Transfer* 67: 469.

50 Baffou, G. and Quidant, R. (2013). Thermo-plasmonics: using metallic nanostructures as nano-sources of heat. *Laser Photonics Rev.* 7: 171.

51 Cui, Y., He, Y., Jin, Y. et al. (2014). Plasmonic and metamaterial structures as electromagnetic absorbers. *Laser Photonics Rev.* 8: 495.

52 Baffou, G. and Quidant, R. (2014). Nanoplasmonics for chemistry. *Chem. Soc. Rev.* 43: 3898.

53 Xue, C. and Li, Q. (2015). *Gold Nanorods in Encyclopedia of Surface and Colloid Science* (ed. P. Somasundaran). Taylor & Francis.

54 Li, Q. (ed.) (2015). *Anisotropic Nanomaterials: Preparation, Properties, and Applications*. Heidelberg: Springer-Verlag.

55 Zhu, M., Baffou, G., Meyerbroker, N., and Polleux, J. (2012). Micropatterning thermoplasmonic gold nanoarrays to manipulate cell adhesion. *ACS Nano* 6: 7227.

56 Wang, Y., Black, K.C.L., Luehmann, H. et al. (2013). Comparison study of gold nanohexapods, nanorods, and nanocages for photothermal cancer treatment. *ACS Nano* 7: 2068.

57 Huang, X., El-Sayed, I.H., Qian, W., and El-Sayed, M.A. (2006). Cancer cell imaging and photothermal therapy in the near-infrared region by using gold nanorods. *J. Am. Chem. Soc.* 128: 2115.

58 Huschka, R., Zuloaga, J., Knight, M.W. et al. (2011). Light-induced release of DNA from gold nanoparticles: nanoshells and nanorods. *J. Am. Chem. Soc.* 133: 12247.

59 Jiang, K., Smith, D.A., and Pinchuk, A. (2013). Size-dependent photothermal conversion efficiencies of plasmonically heated gold nanoparticles. *J. Phys. Chem. C* 117: 27073.

60 Nedyalkov, N.N., Imamova, S.E., Atanasov, P.A. et al. (2011). Interaction of gold nanoparticles with nanosecond laser pulse: nanoparticle heating. *Appl. Surf. Sci.* 257: 5456.

61 Govorov, A.O., Zhang, W., Skeini, T. et al. (2006). Gold nanoparticle ensembles as heaters and actuators: melting and collective plasmon resonances. *Nanoscale Res. Lett.* 1: 84.

62 Hu, M. and Hartland, G.V. (2002). Heat dissipation for Au particles in aqueous solution: relaxation time versus size. *J. Phys. Chem. B* 106: 7029.

63 Baffou, G., Quidant, R., and Girard, C. (2009). Heat generation in plasmonic nanostructures: influence of morphology. *Appl. Phys. Lett.* 94: 153109.

64 Roper, D.K., Ahn, W., and Hoepfner, M. (2007). Microscale heat transfer transduced by surface plasmon resonant gold nanoparticles. *J. Phys. Chem. C* 111: 3636.

65 Chen, H., Shao, L., Ming, T. et al. (2010). Understanding the photothermal conversion efficiency of gold nanocrystals. *Small* 6: 2272.

66 Xue, C. and Li, Q. (2015). Anisotropic gold nanoparticels: preparation, properties, and applications. In: *Anisotropic Nanomaterials: Preparation, Properties, and Applications*, Chapter 3 (ed. Q. Li), 69–118. Heidelberg: Springer-Verlag.

67 Cong, B., Kan, C., Wang, H. et al. (2014). Gold nanorods: near-infrared plasmonic photothermal conversion and surface coating. *J. Mater. Sci. - Chem. Eng.* 2: 20.

68 Bisoyi, H.K. and Li, Q. (2014). *Liquid Crystals, Kirk-Othmer Encyclopedia of Chemical Technology*. New York: Wiley.

69 Li, Q. (ed.) (2014). *Nanoscience with Liquid Crystals: From Self-Organized Nanostructures to Applications*. Springer-Verlag.

70 de Gennes, P.G. and Prost, J. (1993). *The Physics of Liquid Crystals*. Oxford: Oxford University Press.

71 Chandrasekhar, S. (1992). *Liquid Crystals*. Cambridge, UK: Cambridge University Press.

72 Collings, P.J. and Hird, M. (1997). *Introduction to Liquid Crystals: Chemistry and Physics*. London, UK: Taylor & Francis.

73 Warner, M. and Terentjev, E.M. (2003). *Liquid Crystal Elastomers*. New York: Oxford University Press.

74 De Jeu, W.H. (ed.) (2012). *Liquid Crystal Elastomers: Materials and Applications*. Springer-Verlag.

75 Bisoyi, H.K. and Li, Q. (2016). Light-driven liquid crystalline materials: from photo-induced phase transitions and property modulations to applications. *Chem. Rev.* 116: 15089.

76 Li, Q. (ed.) (2012). *Liquid Crystals Beyond Displays: Chemistry, Physics, and Applications*. Hoboken, NJ: Wiley.

77 Wang, L., Gutierrez, K., and Li, Q. (2017). *Photochromic Chiral Liquid Crystal Sensors, Chapter 2 in Liquid Crystalline Sensors* (ed. A. Schenning, G. Crawford and D.J. Broer). CRC Press, Taylor & Francis Group.

78 Bisoyi, H. and Li, Q. (2016). Discotic liquid crystals for self-organizing photovolatics. In: *Nanomaterials for Sustainable Energy*, Chapter 6 (ed. Q. Li), 215–252. Heidelberg: Springer-Verlag.

79 Zheng, Z. and Li, Q. (2016). Self-organized chiral liquid crystalline nanostructures for energy-saving devices. In: *Nanomaterials for Sustainable Energy*, Chapter 14 (ed. Q. Li), 513–558. Heidelberg: Springer-Verlag.

80 Bisoyi, H.K. and Li, Q. (2015). Liquid crystalline anisotropic nanoparticles: from metallic and semiconducting nanoparticles to carbon nanomaterials. In: *Anisotropic Nanomaterials: Preparation, Properties, and Applications*, Chapter 6 (ed. Q. Li), 209–240. Heidelberg: Springer-Verlag.

81 Gutierrez-Cuevas, K.G., Wang, L., Zheng, Z. et al. (2016). Frequency-driven self-organized helical superstructures loaded with mesogen-grafted silica nanoparticles. *Angew. Chem. Int. Ed.* 55: 13090.

82 Montbach, E., Venkataraman, N., Doane, J.W. et al. (2008). Novel optically addressable photochiral displays. *Soc. Inf. Disp. – Dig. Tech. Pap.* 39: 919.

83 Venkataraman, N., Magyar, G., Montbach, E. et al. (2009). Thin flexible photosensitive cholesteric displays. *J. Soc. Inf. Disp.* 17: 869.

84 Li, L., Kang, S., Harden, J. et al. (2008). Nature inspired light-harvesting liquid crystalline porphyrins for organic photovoltaics. *Liq. Cryst.* 35: 233.

85 Zheng, Z., Li, Y., Bisoyi, H.K. et al. (2016). Three-dimensional control of the helical axis of a chiral nematic liquid crystal by light. *Nature* 531: 352.

86 Sun, Q., Dai, L., Zhou, X. et al. (2007). Bilayer- and bulk-heeterojunction solar cells using liquid crystalline porphyrins as donors by solution processing. *Appl. Phys. Lett.* 91: 253505.

87 Zhou, X., Kang, S., Kumar, S. et al. (2008). Self-assembly of porphyrin and fullerene supramolecular complex into highly ordered nanostructure by thermal annealing. *Chem. Mater.* 20: 3551.

88 Zhou, X., Kang, S., Kumar, S., and Li, Q. (2009). Self-assembly of discotic liquid crystal porphyrin into more controllable ordered nanostructure mediated by fluorophobic effect. *Liq. Cryst.* 36: 269.

89 Mathews, M., Zola, R., Hurley, S. et al. (2010). Light-driven reversible handedness inversion in self-organized helical superstructures. *J. Am. Chem. Soc.* 132: 18361.

90 Li, Q., Li, Y., Ma, J. et al. (2011). Directing dynamic control of red, green and blue reflection enabled by a light-driven self-organized helical superstructure. *Adv. Mater.* 23: 5069.

91 Li, Y., Urbas, A., and Li, Q. (2012). Reversible light-directed red, green and blue reflections with thermal stability enabled by a self-organized helical superstructure. *J. Am. Chem. Soc.* 134: 9573.

92 Lin, T.-H., Li, Y., Wang, C.-T. et al. (2013). Red, green and blue reflections enabled in optically tunable self-organized 3D cubic nanostructured thin film. *Adv. Mater.* 25: 5050.

93 Wang, L., Dong, H., Li, Y. et al. (2014). Reversible near-infrared light directed reflection in a self-organized helical superstructure loaded with upconversion nanoparticles. *J. Am. Chem. Soc.* 136: 4480.

94 Zhang, L., Wang, L., Hiremath, U.S. et al. (2017). Dynamic orthogonal switching of a thermoresponsive self-organized helical superstructure. *Adv. Mater.* 29: 1700676.

95 Jau, H.-C., Li, Y., Li, C.-C. et al. (2015). Light-driven wide-range non-mechanical beam steering and spectrum scanning based on a self-organized liquid crystal grating enabled by a chiral molecular switch. *Adv. Opt. Mater.* 3: 166.

96 Zheng, Z., Yuan, C., Hu, W. et al. (2017). Light-patterned crystallographic direction of a self-organized three-dimensional soft photonic crystal. *Adv. Mater.* 29: 1703165.

97 Wang, Y., Singh, G., Agra-Kooijman, D.M. et al. (2015). Room temperature heliconical twist-bend nematic liquid crystal. *CrystEngCommun* 17: 2778.

98 Wang, L., Chen, D., Gutierrez-Cuevas, K. et al. (2017). Optically reconfigurable chiral microspheres of self-organized helical superstructures with handedness inversion. *Mater. Horiz.* 4: 1190.

99 Fan, J., Li, Y., Bisoyi, H.K. et al. (2015). Light-directing omnidirectional circularly polarized reflection from liquid crystal droplets. *Angew. Chem. Int. Ed.* 54: 2160.

100 Wang, Y., Zheng, Z., Bisoyi, H.K. et al. (2016). Thermally reversible full color selective reflection in a self-organized helical superstructure enabled by a bent-core oligomesogen exhibiting twist-bend nematic phase. *Mater. Horiz.* 3: 442.

101 Xiang, J., Li, Y., Li, Q. et al. (2015). Electrically tunable selective reflection of light from ultraviolet to visible and infrared by heliconical cholesterics. *Adv. Mater.* 27: 3014.

102 Wang, L., Dong, H., Li, Y. et al. (2015). Photoluminescence-driven reversible handedness inversion of self-organized helical superstructures enabled by unprecedented near-infrared light nanotransducers. *Adv. Mater.* 27: 2065.

103 White, T., Bricker, R.L., Natarajan, L.V. et al. (2010). Electromechanical and light tunable cholesteric liquid crystals. *Opt. Commun.* 283: 3434.

104 Li, Y., Wang, M., White, T.J. et al. (2013). Azoarenes bearing opposite chiral configurations: light-driven dynamic reversible handedness inversion in self-organized helical superstructure. *Angew. Chem. Int. Ed.* 52: 8925.

105 Li, Y., Xue, C., Wang, M. et al. (2013). Photodynamic chiral molecular switches with thermal stability: from reflection wavelength tuning to handedness inversion of self-organized helical superstructures. *Angew. Chem. Int. Ed.* 52: 13703.

106 Salili, S.M., Xiang, J., Wang, H. et al. (2016). Magnetically tunable selective reflection of light by heliconical cholesterics. *Phys. Rev. E* 94: 042705.

107 Wang, H., Bisoyi, H.K., Urbas, A. et al. (2018). Photochemically and thermally driven full color reflection in a self-organized helical superstructure enabled by a halogen bonded chiral molecular switch. *Angew. Chem. Int. Ed.* 57: 1627.

108 Zheng, Z., Zola, R.S., Bisoyi, H.K. et al. (2017). Dynamic reconfigurable zigzag pattern formation in a soft helical superstructure. *Adv. Mater.* 29: 1701903.

109 Sun, Y., Evans, J.S., Lee, T. et al. (2012). Optical manipulation of shape-morphing elastomeric liquid crystal microparticles doped with gold nanocrystals. *Appl. Phys. Lett.* 100: 241901.

110 Fong, W.-K., Hanley, T.L., Thierry, B. et al. (2012). Controlling the nanostructure of gold nanorod–lyotropic liquid crystalline hybrid materials using near infrared laser irradiation. *Langmuir* 28: 14450.

111 Fong, W.-K., Hanley, T.L., Thierry, B. et al. (2010). Plasmonic nanorods provide reversible control over nanostructure of self-assembled drug delivery materials. *Langmuir* 26: 6136.

112 Fong, W.-K., Hanley, T.L., Thierry, B. et al. (2014). Understanding the photothermal heating effect in non-lamellar liquid crystalline systems, and the design of new mixed lipid systems for photothermal on-demand drug delivery. *Phys. Chem. Chem. Phys.* 16: 24936.

113 Pezzi, L., de Sio, L., Veltri, A. et al. (2015). Photo-thermal effects in gold nanoparticles dispersed in thermotropic nematic liquid crystals. *Phys. Chem. Chem. Phys.* 17: 20281.

114 Liu, X., Wei, R., Hoang, P.T. et al. (2015). Reversible and rapid laser actuation of liquid crystalline elastomer micropillars with inclusion of gold nanoparticles. *Adv. Funct. Mater.* 25: 3022.

115 Yang, H., Liu, J., Wang, Z. et al. (2015). Near-infrared-responsive gold nanorod/liquid crystalline elastomer composites prepared by sequential thiol-click chemistry. *Chem. Commun.* 51: 12126.

116 Gutierrez-Cuevas, K.G., Wang, L., Xue, C. et al. (2015). Near infrared light-driven liquid crystal phase transition enabled by hydrophobic mesogen grafted plasmonic gold nanorods. *Chem. Commun.* 51: 9845.

117 Pezzi, L., de Sio, L., Palermo, G. et al. (2016). Nematic liquid crystals used to control photo-thermal effects in gold nanoparticles. *Proc. SPIE* 9769: 97690C.

118 de Sio, L., Placido, T., Comparelli, R. et al. (2016). Plasmonic photoheating of gold nanorods in thermo-responsive chiral liquid crystals. *J. Opt.* 18: 125005.

119 Wang, L., Gutierrez-Cuevas, K.G., Urbas, A., and Li, Q. (2016). Near-infrared light-directed handedness inversion in plasmonic nanorod-embeded helical superstructure. *Adv. Opt. Mater.* 4: 247.

120 Wang, L., Gutierrez-Cuevas, K.G., Bisoyi, H.K. et al. (2015). NIR light-directing self-organized 3D photonic superstructures loaded with anisotropic plamsonic hybrid nanorods. *Chem. Commun.* 51: 15039.

121 Palermo, G., Cataldi, U., de Sio, L. et al. (2016). Optical control of plasmonic heating effects using reversible photo-alignment of nematic liquid crystals. *Appl. Phys. Lett.* 109: 191906.

122 Palermo, G., Cataldi, U., Pezzi, L. et al. (2017). Thermo-plasmonic effects on E7 nematic liquid crystal. *Mol. Cryst. Liq. Cryst.* 649: 45.

123 Yang, L., Setyowati, K., Li, A. et al. (2008). Reversible infrared actuation of carbon nanotube-liquid crystalline elastomer nanocomposites. *Adv. Mater.* 20: 2271.

124 Ji, Y., Huang, Y.Y., Rungsawang, R., and Terentjev, E.M. (2010). Dispersion and alignment of carbon nanotubes in liquid crystalline polymers and elastomers. *Adv. Mater.* 22: 3436.

125 Li, C., Liu, Y., Lo, C., and Jiang, H. (2011). Reversible white-light actuation of carbon nanotube incorporated liquid crystalline elastomer nanocomposites. *Soft Matter* 7: 7511.

126 Marshall, J.E., Ji, Y., Torras, N. et al. (2012). Carbon-nanotube sensitized nematic elastomer composites for IR-visible photo-actuation. *Soft Matter* 8: 1570.

127 Li, C., Liu, Y., Huang, X., and Jiang, H. (2012). Direct sun-driven artificial heliotropism for solar energy harvesting based on a photo-thermomechanical liquid-crystal elastomer nanocomposites. *Adv. Funct. Mater.* 22: 5166.

128 Kohlmeyer, R.R. and Chen, J. (2013). Wavelength-selective, IR light-driven hinges based on liquid crystalline elastomer composites. *Angew. Chem. Int. Ed.* 52: 9234.

129 Li, C., Huang, X., Li, C., and Jiang, H. (2015). Reversible photo actuated bulk nanocomposite with nematic liquid crystalline elastomer matrix. *Mol. Cryst. Liq. Cryst.* 608: 146.

130 Wang, M., Sayed, S.M., Guo, L. et al. (2016). Multi-stimuli responsive carbon nanotube incorporated polysiloxane azobenzene liquid crystalline elastomer composites. *Macromolecules* 49: 663.

131 Yu, L., Cheng, Z., Dong, Z. et al. (2014). Photomechanical response of polymer-dispersed liquid crystals/graphene oxide nanocomposites. *J. Mater. Chem. C* 2: 8501.

132 Yu, L. and Yu, H. (2015). Light-powered tumbler movement of graphene oxide/polymer nanocomposites. *ACS Appl. Mater. Interfaces* 7: 3834.

133 Quinn, M.D.J., Du, J., Boyd, B.J. et al. (2015). Lipid liquid crystal phase change induced through near-infrared irradiation of entrained graphene particles. *Langmuir* 31: 6605.

134 Quinn, M.D.J., Wang, T., Du, J. et al. (2017). Graphene as a photothermal actuator for control of lipid mesophase structure. *Nanoscale* 9: 341.

135 Yang, Y., Zhan, W., Peng, R. et al. (2015). Graphene-enabled superior and tunable photomechanical actuation in liquid crystalline elastomer nanocomposites. *Adv. Mater.* 27: 6376.

136 Li, C., Liu, Y., Huang, X. et al. (2015). Light actuation of graphene-oxide incorporated liquid crystalline elastomer nanocomposites. *Mol. Cryst. Liq. Cryst.* 616: 83.

137 Wang, L., Bisoyi, H.K., Zheng, Z. et al. (2017). Stimuli-directed self-organized chiral superstructures for adaptive windows enabled by mesogen-functionalized graphene. *Mater. Today* 20: 230.

138 Vallooran, J.J., Handschin, S., Bolisetty, S., and Mezzenga, R. (2012). Twofold light and magnetic responsive behavior in nanoparticle-lyotropic liquid crystal systems. *Langmuir* 28: 5589.

139 Ono, H. and Kawatsuki, N. (1997). Photothermal response characterstics of host-guest liquid crystals. *Jpn. J. Appl. Phys.* 36: 761.

140 Ono, H., Harato, Y., and Kawatsuki, N. (1998). Photothermal effects in liquid crystals on dye-doped polymer films. *J. Appl. Phys.* 83: 4957.

141 Guo, L., Liu, M., Sayed, S.M. et al. (2016). A calamitic mesogenic near-infrared absorbing croconaine dye/liquid crystalline elastomer composite. *Chem. Sci.* 7: 4400.

142 Liu, W., Guo, L., Lin, B. et al. (2016). Near-infrared responsive liquid crystalline elastomers containing photothermal conjugated polymers. *Macromolecules* 49: 4023.

143 Gelebart, A.H., Vantomme, G., Meijer, E.W., and Broer, D.J. (2017). Mastering the photothermal effect in liquid crystal networks: a general approach for self-sustained mechanical oscillators. *Adv. Mater.* 29: 1606712.

144 Liu, L., Liu, M., Deng, L. et al. (2017). Near-infrared chromophore functionalized soft actuator with ultrafast photoresponsive speed and superior mechanical property. *J. Am. Chem. Soc.* 139: 11333.

145 Li, Z., Yang, Y., Wang, Z. et al. (2017). Polydopamine nanoparticles doped in liquid crystal elastomers for producing dynamic 3D structures. *J. Mater. Chem. A* 5: 6740.

146 Tian, H., Wang, Z., Chen, Y. et al. (2018). Polydopamine-coated main-chain liquid crystal elastomer as optically driven artificial muscle. *ACS Appl. Mater. Interfaces* 10: 8307.

147 Paul, D.R. and Robeson, L.M. (2008). Polymer nanotechnology: nanocomposites. *Polymer* 49: 3187.

148 Moniruzzaman, M. and Winey, K.I. (2006). Polymer nanocomposites containing carbon nanotubes. *Macromolecules* 39: 5194.

149 Yuan, Z., Xiao, X., Li, J. et al. (2018). Self-assembled graphene-based architectures and their applications. *Adv. Sci.* 5: 1700626.

150 Kumar, S.K., Benicewicz, B.C., Vaia, R.A., and Winey, K.I. (2017). 50th anniversary perspective: are polymer nanocomposites practical for applications? *Macromolecules* 50: 714.

151 Ionov, L. (2015). Polymer actuators. *Langmuir* 31: 5015.

152 Lu, S., Ahir, S., Valesco, V. et al. (2009). Photo-mechanical actuation of carbon nanotubes: mechanisms and applications in micro and nano-devices. *J. Micro - Nano Mechatron.* 5: 29.

153 Koerner, H., Price, G., Pearce, N.A. et al. (2004). Remotely actuated polymer nanocomposites - stress-recovery of carbon-nanotube-filled thermoplastic elastomers. *Nat. Mater.* 3: 115.

154 Ahir, S.V. and Terentjev, E.M. (2005). Photomechanical actuation in polymer-nanotube composites. *Nat. Mater.* 4: 491.

155 Ahir, S.V., Squires, A.M., Tajbakhsh, A.R., and Terentjev, E.M. (2006). Infrared actuation in aligned polymer-nanotube composites. *Phys. Rev. E* 73: 085420.

156 Lu, S. and Panchapakesan, B. (2007). Photomechanical responses of carbon nanotube/polymer actuators. *Nanotechnology* 18: 305502.

157 Miyako, E., Nagata, H., Hirona, K., and Hirotsu, T. (2008). Carbon-nanotube-polymer composite for light-driven microthermal control. *Angew. Chem. Int. Ed.* 47: 3610.

158 Czanikova, K., Krupa, I., Iicikova, M. et al. (2012). Photo-actuating materials based on elastomers and modified carbon nanotubes. *J. Nanophotonics* 6: 063522.

159 Czanikova, K., Torras, N., Esteve, J. et al. (2013). Nanocomposite photoactuators based on an ethylene vinyl acetate copolymer filled with carbon nanotubes. *Sens. Actuators, B* 186: 701.

160 Tang, B., Wang, Y., Qiu, M., and Zhang, S. (2014). A full-band sunlight-driven carbon nanotube/PEG/SiO$_2$ composites for solar energy storage. *Sol. Energy Mater. Sol. Cells* 123 (7).

161 Ilcikova, M., Mrlik, M., Sedlacek, T. et al. (2014). Synthesis of photoactuating acrylic thermoplastic elastomers containing diblock copolymer-grafted carbon nanotubes. *ACS Macro Lett.* 3: 999.

162 Shen, Y., Skirtach, A.G., Seki, T. et al. (2010). Assembly of fullerene-carbon nanotubes: temperature indicator for photothermal conversion. *J. Am. Chem. Soc.* 132: 8566.

163 Asanuma, H., Subedi, P., Hartmann, J. et al. (2013). Nanoplasmonic modification of the local morphology, shape, and wetting properties of nanoflake microparticles. *Langmuir* 29: 7464.

164 Kim, H., Abdala, A.A., and Macosko, C.W. (2010). Graphene/polymer nanocomposites. *Macromolecules* 43: 6515.

165 Liang, J., Xu, Y., Huang, Y. et al. (2009). Infrared-triggered actuators from graphene-based nanocomposites. *J. Phys. Chem. C* 113: 9921.

166 Loomis, J., King, B., and Panchapakesan, B. (2012). Layer dependent mechanical responses of graphene composites to near-infrared light. *Appl. Phys. Lett.* 100: 073108.

167 Loomis, J., Fan, X., Khosravi, F. et al. (2013). Graphene/elastomer composite-based photothermal nanopositioners. *Sci. Rep.* 3: 1900.

168 Ansari, S., Neelanchery, M.M., and Ushus, D. (2013). Graphene/poly(styrene-*b*-isoprene-*b*-styrene) nanocomposite optical actuators. *J. Appl. Polym. Sci.* 130: 3902.

169 Meng, D., Yang, S., Guo, L. et al. (2014). The enhanced photothermal effect of graphene/conjugated polymer composites: photoinduced energy transfer and applications in photocontrolled switches. *Chem. Commun.* 50: 14345.

170 Muraldharan, M.N., Shinu, K.P., and Seema, A. (2016). Optically triggered actuation in chitosan/reduced graphene oxide nanocomposites. *Carbohydr. Polym.* 144: 115.

171 Leeladhar, P., Raturi, A., and Kumar, J.P.S. (2017). Graphene-polydimethylsiloxane/chromium bilayer-based flexible, reversible, and large bendable photomechanical actuators. *Smart Mater. Struct.* 26: 095030.

172 Robinson, J.T., Tabakman, S.M., Liang, Y. et al. (2011). Ultrasmall reduced graphene oxide with high near-infrared absorbance for photothermal therapy. *J. Am. Chem. Soc.* 133: 6825.

173 Feng, Y., Qin, M., Guo, H. et al. (2013). Infrared actuated recovery of polyurethane filled by reduced graphene oxide/carbon nanotube hybrids with high energy density. *ACS Appl. Mater. Interfaces* 5: 10882.

174 Niu, D., Jiang, W., Liu, H. et al. (2016). Reversible bending behaviors of photomechanical soft actuators based on graphene nanocomposites. *Sci. Rep.* 6: 27366.

175 Yang, J., Choi, J., Bang, D. et al. (2011). Convertible organic nanoparticles for near-infrared photothermal ablation of cancer cells. *Angew. Chem. Int. Ed.* 50: 441.

176 Zhou, J., Lu, Z., Zhu, X. et al. (2013). NIR photothermal therapy using polyaniline nanoparticles. *Biomaterials* 34: 9584.

177 Geng, J., Sun, C., Liu, J. et al. (2015). Biocompatible conjugated polymer nanoparticles for efficient photothermal tumor therapy. *Small* 11: 1603.

178 Lyu, Y., Xie, C., Chechetka, S.A. et al. (2016). Semiconducting polymer nanobioconjugates for targeted photothermal activation of neurons. *J. Am. Chem. Soc.* 138: 9049.

179 Lyu, Y., Fang, Y., Miao, Q. et al. (2016). Intraparticle molecular orbital engineering of semiconducting polymer nanoparticles as amplified theranostics for in vivo photoacoustic imaging and photothermal therapy. *ACS Nano* 10: 4472.

180 Cao, Y., Dou, J.H., Zhao, N. et al. (2017). Highly efficient NIR-II photothermal conversion based on an organic conjugated polymer. *Chem. Mater.* 29: 718.

181 Satarkar, N.S., Biswal, D., and Hilt, J.Z. (2010). Hydrogel nanocomposites: a review of applications as remote controlled biomaterials. *Soft Matter* 6: 2364.

182 Thoniyot, P., Tan, M.J., Karim, A.A. et al. (2015). Nanoparticle-hydrogel composites: concepts, design, and applications of these promising, multi-functional materials. *Adv. Sci.* 2: 1400010.

183 Ionov, L. (2014). Hydrogel-based actuators: possibilities and limitations. *Mater. Today* 17: 494.

184 Cametti, M. and Dzolic, Z. (2014). New frontiers in hybrid materials: nobel metal nanoparticles-supramolecular gel systems. *Chem. Commun.* 50: 8273.

185 Leijten, J., Seo, J., Yue, K. et al. (2017). Spatially and temporally controlled hydrogels for tissue engineering. *Mater. Sci. Eng., R* 119: 1.

186 Mebrouk, K., Debnath, S., Fourmigue, M., and Camerel, F. (2014). Photothermal control of the gelation properties of nickel bis(dithiolene) metallogelators under near-infrared irradiation. *Langmuir* 30: 8592.

187 Wang, C., Wang, X., Dong, K. et al. (2016). Injectable and responsively degradable hydrogel for personalized photothermal therapy. *Biomaterials* 104: 129.

188 Zheng, Z., Hu, J., Wang, H. et al. (2017). Dynamic softening or stiffening a supramolecular gel by ultraviolet or near-infrared light. *ACS Appl. Mater. Interfaces* 9: 24511.

189 Okano, K., Nogami, A., and Asakura, K. (2014). High-strength gel actuator driven by a photothermal effect. *Polym. J.* 46: 827.

190 Mohamed, M.B., Ahmadi, T.S., Link, S. et al. (2001). Hot electron and phonon dynamics of gold nanoparticles embedded in a gel matrix. *Chem. Phys. Lett.* 343: 55.

191 Kim, J.-H. and Lee, T.R. (2004). Thermo- and pH-responsive hydrogel-coated gold nanoparticles. *Chem. Mater.* 16: 3647.

192 Kawano, T., Niidome, Y., Mori, T. et al. (2009). PNIPAM gel-coated gold nanorods for targeted delivery responding to a near-infrared laser. *Bioconjugate Chem.* 20: 209.

193 Gramlich, W.M., Holloway, J.L., Rai, R., and Burdick, J.A. (2014). Transdermal gelation of methacrylated macromers with near-infrared light and gold nanorods. *Nanotechnology* 25: 014004.

194 Stower, R.S., Allen, S.C., and Suggs, L.J. (2015). Dynamic phototuning of 3D hydrogel stiffness. *Proc. Natl. Acad. Sci. U.S.A.* 112: 1953.

195 Collins, S.S.E., Wei, X., McKenzie, T.G. et al. (2016). Single gold nanorod charge modulation in an ion gel device. *Nano Lett.* 16: 6863.

196 Park, H., Yang, S., Kang, J.Y., and Park, M.-H. (2016). On-demand drug delivery system using micro-organogels with gold nanorods. *ACS Med. Chem. Lett.* 7: 1087.

197 Sershen, S.R., Mensing, G.A., Ng, M. et al. (2005). Independent optical control of microfluidic valves formed from optomechanically responsive nanocomposite hydrogels. *Adv. Mater.* 17: 1366.

198 Shiotani, A., Mori, T., Niidome, T. et al. (2007). Stable incorporation of gold nanorods into *N*-isopropylacrylamide hydrogels and their rapid shrinkage induced by near-infrared laser irradiation. *Langmuir* 23: 4012.

199 Erdogan, H., Sakalak, H., Yazuv, M.S., and Demirel, G. (2013). Laser-triggered degelation control of gold nanoparticle embedded peptide organogels. *Langmuir* 29: 6975.

200 Zhou, Y., Hauser, A.W., Bende, N.P. et al. (2016). Waveguiding microactuators based on a photothermally responsive nanocomposite hydrogel. *Adv. Funct. Mater.* 26: 5447.

201 Lo, C.-W., Zhu, D., and Jiang, H. (2011). An infrared-light responsive graphene-oxide incorporated poly(*N*-isopropylacrylamide)hydrogel nanocomposite. *Soft Matter* 7: 5604.

202 Zhang, X., Pint, C.L., Lee, M.H. et al. (2011). Optically- and thermally-responsive programmable materials based on carbon nanotube-hydrogel polymer composites. *Nano Lett.* 11: 3239.

203 Zhang, E., Wang, T., Hong, W. et al. (2014). Infrared-driving actuation based bilayer graphene oxide-poly(*N*-isopropylacrylamide) nanocomposite hydrogels. *J. Mater. Chem. A* 2: 15633.

204 Zhu, C.-H., Lu, Y., Peng, J. et al. (2012). Photothermally sensitive poly(*N*-isopropylacrylamide)/graphene oxide nanocomposite hydrogels as remote light-controlled liquid microvalves. *Adv. Funct. Mater.* 22: 4017.

205 Hsiao, C.-W., Chuang, E.-Y., Chen, H.-L. et al. (2015). Photothermal tumor ablation in mice with repeated therapy sessions using NIR-absorbing micellar hydrogels formed in situ. *Biomaterials* 56: 26.

206 Fujigaya, T., Moromoto, T., Niidome, Y., and Nakashima, N. (2008). NIR lase-driven reversible volume phase transition of single-walled carbon nanotube/poly(*N*-isopropylacrylamide)composite gels. *Adv. Mater.* 20: 3610.

207 Li, W., Wang, J., Ren, J., and Qu, X. (2013). 3D graphene oxide-polymer hydrogel: near-infrared light-triggered active scaffold for reversible cell capture and on-demand release. *Adv. Mater.* 25: 6737.

208 Wang, E., Desai, M.S., and Lee, S.-W. (2013). Light-controlled graphene-elastin composite hydrogel actuators. *Nano Lett.* 13: 2826.

209 Cong, H.-P., Qiu, J.-H., and Yu, S.-H. (2015). Thermoresponsive poly(*N*-isopropylacrylamide)/graphene/Au nanocomposite hydrogel for water treatment by a laser-assisted approach. *Small* 11: 1165.

210 Kim, D., Lee, H.S., and Yoon, J. (2016). Highly bendable bilayer-type photo-actuators comprising of reduced graphene oxide dispersed in hydrogels. *Sci. Rep.* 6: 20921.

211 Satarkar, N.S., Zhang, W., Eitel, R.E., and Hilt, J.Z. (2009). Magnetic hydrogel nanocomposites as remote controlled microfluidic valves. *Lab Chip* 9: 1773.

212 Khoshmanesh, K., Tang, S.-Y., Zhu, J.Y. et al. (2017). Liquid metal enabled microfluidics. *Lab Chip* 17: 974.

213 Dickey, M.D. (2014). Emerging applications of liquid metals featuring surface oxides. *ACS Appl. Mater. Interfaces* 6: 18369.

214 Yoon, J., Bian, P., Kim, J. et al. (2012). Local switching of chemical patterns through light-triggered unfolding of creased hydrogel surfaces. *Angew. Chem. Int. Ed.* 51: 7146.

215 Lee, E., Lee, H., Yoo, S.I., and Yoon, J. (2014). Photothermally triggered fast responding hydrogels incorporating a hydrophobic moiety for light-controlled microvalves. *ACS Appl. Mater. Interfaces* 6: 16949.

216 Zhu, C.H., Lu, Y., Chen, J.-F., and Yu, S.-H. (2014). Photothermal poly(N-isopropylacrylamide)/Fe_3O_4 nanocomposite hydrogel as a movable position heating source under remote control. *Small* 10: 2796.

217 Lee, E., Kim, D., Kim, H., and Yoon, J. (2015). Photothermally driven fast responding photo-actuators fabricated with comb-type hydrogels and magnetite nanoparticles. *Sci. Rep.* 5: 15124.

218 Lim, D., Lee, E., Kim, H. et al. (2015). Multi stimuli-responsive hydrogel microfibers containing magnetite nanoparticles prepared using microcapillary devices. *Soft Matter* 11: 1606.